Synthesis and Characterization of Enantiomerically Pure *cis*- and *trans*-3-Fluoro-2,4-dioxa-7-aza-3-phosphadecalin 3-Oxides as Acetylcholine Mimetics and Inhibitors of Acetylcholinesterase

by **Michael Wächter** and **Peter Rüedi***

Organisch-chemisches Institut der Universität Zürich, Winterthurerstrasse 190, CH-8057 Zürich (phone: +41-44-8215579)

The title compounds, the *P(3)*-axially and *P(3)*-equatorially substituted *cis*- and *trans*-configured 7-benzyl-3-fluoro-2,4-dioxa-7-aza-3-phosphadecalin 3-oxides (= 7-benzyl-3-fluoro-2,4-dioxa-7-aza-3-phosphabicyclo[4.4.0]decane 3-oxides = 5-benzyl-2-fluorohexahydro-4*H*-1,3,2-dioxaphosphorino[5,4-*b*]-pyridine 2-oxides) were prepared (ee > 99%) and fully characterized (*Schemes 2* and *4*). The absolute configurations were established from that of their precursors, the enantiomerically pure *cis*- and *trans*-1-benzyl-3-hydroxypiperidine-2-methanols which were unambiguously assigned. Being configuratively fixed and conformationally constrained phosphorus analogues of acetylcholine, they mimic rotamers of acetylcholine and are suitable probes for the investigation of molecular interactions with acetylcholinesterase. As determined by kinetic methods, the compounds are irreversible inhibitors of the enzyme displaying significant stereoselectivity.

1. Introduction. – In preceding reports, we have presented the synthesis and characterization of the enantiomerically pure *P*(*3*)-axially and *P(3)*-equatorially substituted *cis*- and *trans*-configured 3-fluoro-2,4-dioxa-9-aza-3-phospha- (type **I**) [1], 3-fluoro-2,4-dioxa-8-aza-3-phospha- (type **II**) [2], and 3-fluoro-2,4-dioxa-3-phosphadecalin 3-oxides (type **IV**) [3] (*Scheme 1*). Continuing our investigations on the inhibition of serine hydrolases (chymotrypsin, acetylcholinesterase) by decalin-type organophosphates, we discuss the preparation and characterization of the isomeric enantiomerically pure 7-benzyl-3-fluoro-2,4-dioxa-7-aza-3-phosphadecalin 3-oxides (= 7-benzyl-3-fluoro-2,4-dioxa-7-aza-3-phosphabicyclo[4.4.0]decane 3-oxides = 5-benzyl-2-fluorohexahydro-4*H*-1,3,2-dioxaphosphorino[5,4-*b*]pyridine 2-oxides **13** and **14** (type **III**, *cf. Schemes 1* and *4*)) [4]. The compounds are mimetics of rotamers of acetylcholine (= 2-(acetyloxy)-*N*,*N*,*N*-trimethylethanaminium; ACh) and as such are considered to be suitable probes for the investigation of molecular interactions with acetylcholinesterase (AChE) [5] and the stereochemical course of the inhibition reaction by ^{31}P-NMR spectroscopy [4][6–8].

2. Synthesis and Characterization of the Precursors. – 2.1. *Preparation of the Enantiomerically Pure* (+)- *and* (−)-trans- *and (+)- and* (−)-cis-*1-Benzyl-3-hydroxypiperidine-2-methanols* ((+)- and (−)-**4**, and (+)- and (−)-**5**, resp.). Following the protocol for the preparation of the racemic compounds [9], 3-hydroxypyridine-2-methanol (**1**) was converted by a six-step reaction sequence followed by chromatographic separation (SiO_2) of the diastereoisomers to the key intermediates (±)-*trans*-

Scheme 1

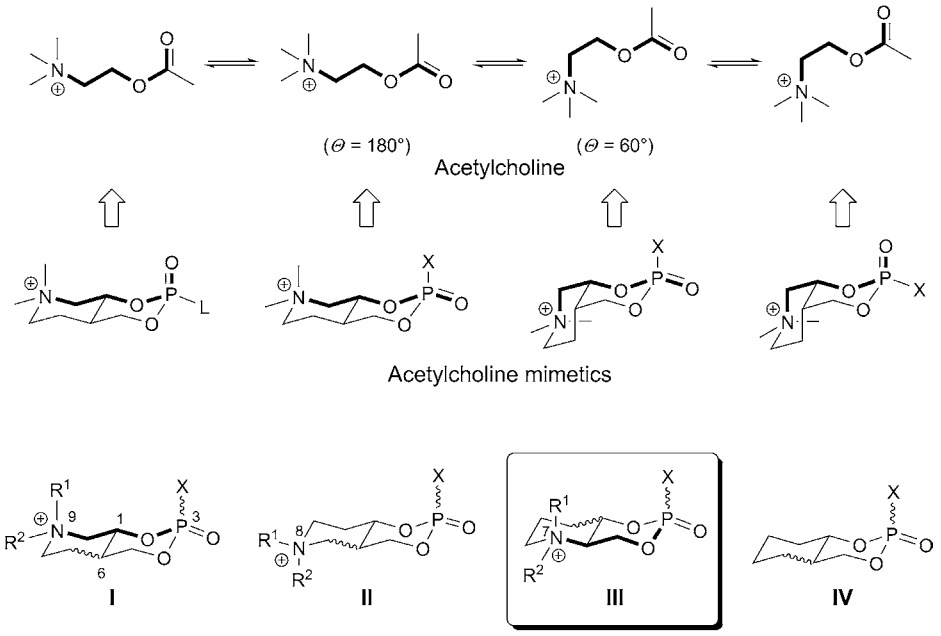

[a]) Structural types **I** – **IV**: *cis*- and *trans*-, and axially, and equatorially P-substituted isomers for each type
X = Selected electron-withdrawing group, *e.g.*, F, Cl, 4-nitrophenoxy, 2,4-dinitrophenoxy or amino acid derivatives (model compounds)
R^1, R^2 = (*tert.* amines, free bases) = H, Me, CH_2Ph; $R^1 = R^2$ or $R^1 \neq R^2$

and (±)-*cis*-[3-(acetyloxy)-1-benzylpiperidin-2-yl]methyl 2,2-dimethylpropanoates ((±)-**2** and (±)-**3**; *Scheme 2*). Preparative HPLC (*Chiralcel® OD*) afforded the optically active diesters (+)-**2** ($k' = 1.68$, ee > 99%), (−)-**2** ($k' = 2.08$, ee > 99%), (+)-**3** ($k' = 0.74$, ee > 99%), and (−)-**3** ($k' = 1.01$, ee > 99%). Hydrolysis of the respective diesters gave the 1-benzyl-3-hydroxypiperidine-2-methanols (+)-**4** ($[\alpha]_D = +43.5$, ee > 99%), (−)-**4** ($[\alpha]_D = -43.7$, ee > 99%), (+)-**5** ($[\alpha]_D = +21.3$, ee > 99%), and (−)-**5** ($[\alpha]_D = -21.5$, ee > 99%) (*Scheme 2*)[1])

2.2. *The Absolute Configurations of the Diols (+)- and (−)-**4**, and (+)- and (−)-**5**.* The absolute configurations of the diols (+)- and (−)-**4**, and (+)- and (−)-**5** were inferred by the high-field ^{1}H-NMR application of the *Mosher* method [10] and its extension to the bis-MTPA derivatives **6**–**9** as recently reported [11]. Esterification of (−)- and (+)-**4** with (+)-(*S*)-MTPA-Cl (=(+)-(*S*)-α-methoxy-α-(trifluoromethyl)benzeneacetyl chloride) afforded the bis-(*R*)-esters **6a** and **7a**, and the corresponding bis-(*S*)-esters **6b** and **7b** were isolated after reaction of (−)- and (+)-**4** with (−)-(*R*)-MTPA-Cl. The same procedure was performed with (−)- and (+)-**5** to yield the bis-(*R*)-esters **8a** and **9a**, and the bis-(*S*)-esters **8b** and **9b** (*Scheme 2*).

---

[1]) The $[\alpha]_D$ values were determined in EtOH (c = between 0.55 and 1.28), ee > 99%.

Scheme 2[1])

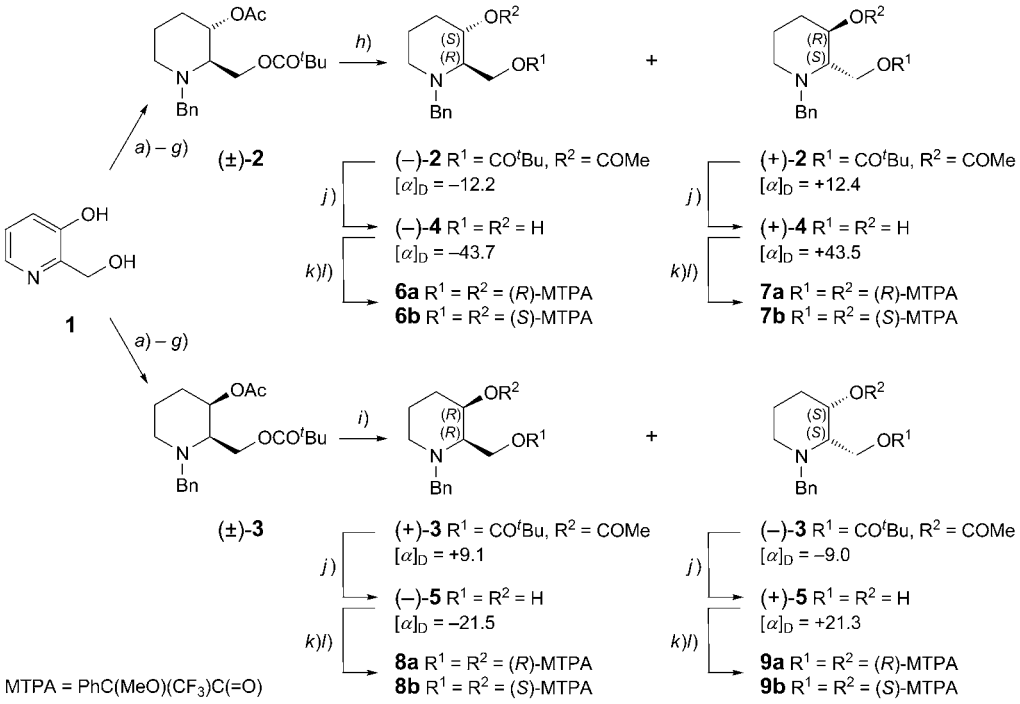

a) H_2, Rh/Alox, 60 bar, H_2O, pH 3, 35°. *b*) BnBr, K_2CO_3, EtOH, reflux. *c*) ^{t}BuCOCl, pyridine, –20°. *d*) $(COCl)_2$, DMSO, CH_2Cl_2, –60°. *e*) $NaBH_4$, EtOH, –15° (*cis*/*trans* 1:1). *f*) Ac_2O, pyridine, r.t. *g*) CC (SiO_2, hexane/AcOEt) (*a*)–*g*) as in Scheme 4 in [9]). *h*) Prep. HPLC (*Chiralcel® OD*, hexane/(±)-2-BuOH). *i*) Prep. HPLC (*Chiralcel® OD*, hexane/^{i}PrOH). *j*) KOH, EtOH/H_2O, r.t. *k*) (–)-(*R*)- or (+)-(*S*)-MTPA-Cl, resp., Et_3N, *N*,*N*-dimethylpyridin-4-amine (DMAP), CH_2Cl_2, r.t. (note: (*R*)-MTPA-Cl yields the (*S*)-MTPA ester and *vice versa*). *l*) CC (SiO_2, hexane/Et_2O).

In the *trans*-series, the analysis of the ^{1}H-NMR data led to the assignment of the absolute configurations at C(3) as (3*R*) and (3*S*) for (+)-**4** and (–)-**4**, respectively. The results were self-contained, and the $\Delta\delta$ values ($=\delta(S)-\delta(R)$) of the diagnostically relevant signals were consistent: for the couple **6a**/**6b**, we observed $\Delta\delta$(H–C(2)) = –0.16, $\Delta\delta(H_{eq}$–C(4)) = +0.15, and $\Delta\delta(CH_2(5)) = -0.05$, and the inverse was found for the couple **7a**/**7b** (see *Exper. Part*)[2]). The fact that $\Delta\delta$(H–C(3)) = 0 for the couples **6a**/**6b** and **7a**/**7b** is indicative for the ideal conformation of the MTPA moiety[3]) and the reliability of the experiment. As a consequence, the absolute configurations of the

[2]) Since **6a** = *ent*-**7b** and **6b** = *ent*-**7a**, **6a** (2′*R*,2*R*,3*S*) and **7b** (2′*S*,2*S*,3*R*), as well as **6b** (2′*S*,2*R*,3*S*) and **7a** (2′*R*,2*S*,3*R*) have identical NMR spectra.

[3]) The theoretical prerequisite for the success and reliability of the ^{1}H-NMR *Mosher* experiments is that the MTPA moiety adopts an idealized conformation where the H-atom at the decisive stereogenic center C(3), the C=O, and the CF_3 groups lie in the same plane in a relative *syn*-arrangement [10]. Therefore, an essential quality factor for the experiment is the equal chemical shift ($\Delta\delta = 0$) for H–C(3) in both the (*R*)- and the (*S*)-MTPA derivatives.

trans-3-hydroxypiperidine-2-methanols (+)-**4** and (−)-**4** were assigned as (2*S*,3*R*), and (2*R*,3*S*), respectively.

In the conformationally flexible *cis*-series **8a**/**8b** and **9a**/**9b**, the reliability of the interpretation was *a priori* reduced due to $\Delta\delta$(H–C(3)) = ± 0.072 for the couples **8a**/**8b** and **9a**/**9b**. According to the ^{1}H-NMR spectra, the MTPA–O group at C(3) is axial, and the magnitudes of the respective vicinal couplings suggested that the conformation is not an ideal chair[4]). However, the $\Delta\delta$ values of the diagnostically relevant signals were as consistent as in the *trans*-series: $\Delta\delta$(H–C(2)) = + 0.04, $\Delta\delta$(CH_2(4)) = − 0.09, and $\Delta\delta$(CH_2(5)) = − 0.07 for the couple **8a**/**8b**, and *vice versa* for **9a**/**9b** (see *Exper. Part*). The low quality factor ($\Delta\delta$(H–C(3)) seems to reflect the sterical impact of the MTPA–OCH_2 moiety at C(2) and the conformational uncertainty. However, taking the consistency of the $\Delta\delta$ values into account, the absolute configurations of the *cis*-3-hydroxypiperidine-2-methanols (+)-**5** and (−)-**5** were inferred as (3*S*) and (3*R*), and as a consequence, as (2*S*,3*S*), and (2*R*,3*R*), respectively[5]).

Further support for this assignment was provided by a modified *Mosher* approach: Esterification of (±)-**10** with (+)-(*S*)-MTPA-Cl and preparative HPLC separation (*Chiralcel® OD*) afforded the 2-[(pivaloyloxy)methyl]-substituted (*R*)-MTPA esters **11** and **12** (*Scheme 3*). The ^{1}H-NMR analysis of **11** and **12** showed the MTPA–O group at C(3) to be equatorial[6]), and the quality factor ($\Delta\delta$(H–C(3)) = + 0.022) was indicative for a nearly idealized conformation of the MTPA moiety and the enhanced reliability of the experiment. As depicted in *Fig. 1*, the arrangement of the bulky substituents in **12** only resulted in an small paramagnetic shift of H–C(2) ($\Delta\delta$ = − 0.01), whereas the H-atoms in the sphere of influence of the (*R*)-MTPA phenyl group in **11** were shielded with respect to **12**, in particular CH_2(4) ($\Delta\delta(H_{ax}–C(4))$ = + 0.07, $\Delta\delta(H_{eq}–C(4))$ = + 0.03)[7]). The identity of the parent diols was verified by hydrolysis of the diastereoisomers **11** and **12** that afforded (−)-**5** and (+)-**5**, respectively (*Scheme 3*). Hence, the absolute configurations were in accord with the previous assignment.

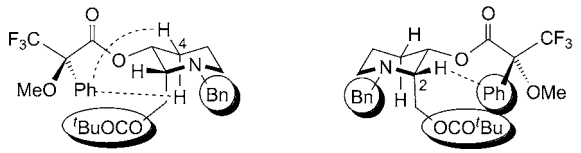

11 **12**

Fig. 1. *Shielding effects of the* (R)*-MTPA phenyl group in* **11** *and* **12**

---

4) H–C(2) is equatorial, H–C(3) is axial (**9a**: ^3J(2,3) = 4.0, ^3J(3,4ax) = 7.8, and ^3J(3,4eq) = 4.0 Hz; **9b**: ^3J(2,3) = 4.0, ^3J(3,4ax) = 7.6, and ^3J(3,4eq) = 4.0 Hz).

5) Subtle differential reasoning, including the shielding effects exerted on H_{ax}–C(6), H_{eq}–C(6) and $PhCH_2$ (H_A, H_B), suggests the most probable conformation. Although it deviates from the ideal arrangement [10], the *Mosher* experiment can be interpreted in terms of the absolute configuration as indicated [4].

6) H–C(2) is equatorial, H–C(3) is axial (**11**: ^3J(2,3) = 3.3, and ^3J(3,4ax) = 6.6, and ^3J(3,4eq) = 3.3 Hz; **12**: ^3J(2,3) = 3.3, and ^3J(3,4ax) = 6.9, and ^3J(3,4eq) = 3.3 Hz).

7) For the reason of simplicity, chair conformations are depicted for **11** and **12** although the vicinal couplings suggest that they deviate from ideal chairs. However, this imprecision does not affect the basic argumentation.

Scheme 3

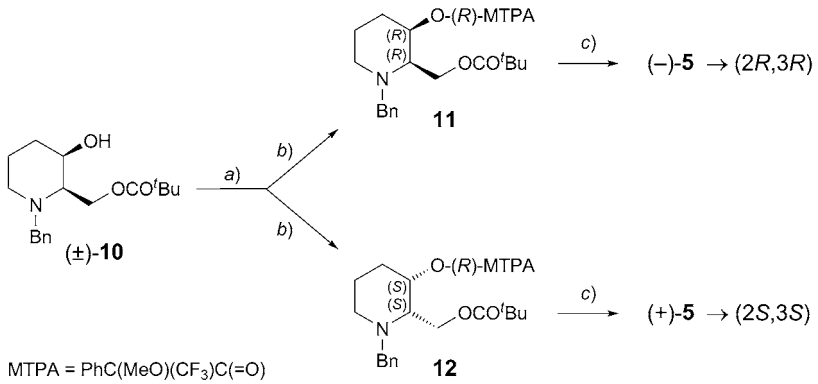

a) (+)-(*S*)-MTPA-Cl, Et_3N, *N*,*N*-dimethylpyridin-4-amine (DMAP), CH_2Cl_2, r.t. *b*) Prep. HPLC (*Chiralcel® OD*, hexane/^{i}PrOH). *c*) KOH, EtOH/H_2O.

Conclusive evidence for the absolute configuration of (+)- and (−)-**4**, and (+)- and (−)-**5** was provided by the X-ray crystallographic analysis (*Sect. 3.3*) of the 7-aza-3-phosphadecalins (−)-**13a** (*Fig. 2*) and (+)-**14a** (*Fig. 3*). This is the first account of the full characterization of the isomeric 1-benzyl-3-hydroxypiperidine-2-methanols **4** and **5**[8]).

3. Synthesis and Characterization of the 7-Benzyl-3-fluoro-2,4-dioxa-7-aza-3-phosphadecalins. – 3.1. *2,4-Dioxa-7-aza-3-phosphadecalin 3-Oxides* **13** *and* **14**. Applying our reliable protocol [9], the enantiomerically pure *trans*-7-benzyl-3-fluoro-2,4-dioxa-7-aza-3-phosphadecalins **13** (*Scheme 4*) were prepared from (+)- or (−)-**4** by reaction with $POCl_2F$ and chromatographic separation of the resulting *P(3)*-epimer mixture (axial/equatorial *ca.* 1.5 : 1) into the pure axial epimers (+)- and (−)-**13a** and equatorial epimers (+)- and (−)-**13b**. Similarly, starting from (+)- or (−)-**5**, the *cis*-7-benzyl-3-fluoro-2,4-dioxa-9-aza-3-phosphadecalins (+)- and (−)-**14a**, and (+)- and (−)-**14b** were obtained (*Scheme 4*)[9]). The NMR data of the 7-aza-3-phosphadecalins

---

[8]) The (2*S*,3*R*)-configuration has been assigned to the *trans*-configured 1-benzyl- and 1-methyl-3-hydroxypiperidine-2-methanols [12] but no chiroptical data were reported. In connection with investigations on 3-hydroxypipecolic acid analogues, piperidine alkaloids, and aza-carbohydrates, the closely related 3-hydroxypiperidine-2-methanols [13], 1-butyl-3-hydroxypiperidine-2-methanols [14], and *tert*-butyl 3-hydroxy-2-(hydroxymethyl)piperidine-1-carboxylates [15] have been described. In the *cis*-series, the signs of the optical rotation are consistent and equal to those of (+)- and (−)-**5** ((2*S*,3*S*): $[\alpha]_D > 0$; (2*R*,3*R*): $[\alpha]_D < 0$), whereas they differ in the *trans*-series. The latter fact might be due to conformational impacts as *tert*-butyl (2*S*,3*R*)-3-hydroxy-2-(hydroxymethyl)piperidine-1-carboxylate adopts the unexpected diaxial arrangement of the substituents [16]. However, the only report that presents all 4 stereoisomers [14] contains several inconsistencies: The enantiomeric *trans*-1-butyl-3-hydroxypiperidine-2-methanols are both dextrorotatory ((2*R*,3*S*): $[\alpha]_D = +2.7$; (2*S*,3*R*): $[\alpha]_D = +13.3$), and the *cis*-1-butyl-3-hydroxypiperidine-2-methanols have inverted signs ((2*R*,3*R*): $[\alpha]_D > 0$; (2*S*,3*S*): $[\alpha]_D < 0$) with respect to all other accounts [13][15]. See also our discussions on configurational and chiroptical inconsistencies in the 1-substituted 4-hydroxypiperidine-3-methanols [11] and the 3-hydroxypiperidine-4-methanols [17].

[9]) The $[\alpha]_D$ values were determined in acetone (c = between 0.26 and 0.38), ee > 99%.

Scheme 4[9])

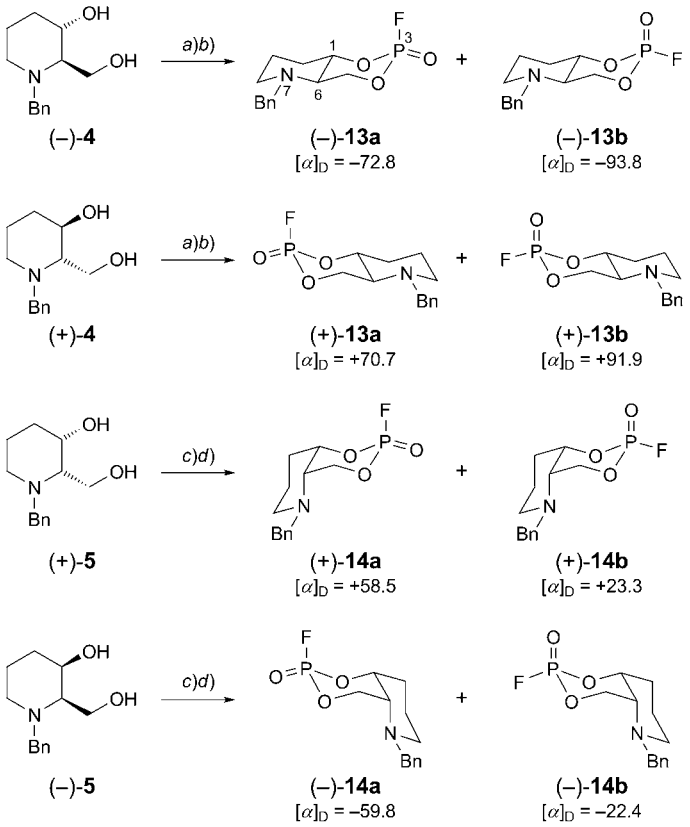

a) $Cl_2P(O)F$, Et_3N, Et_2O, $< 0°$. *b*) CC (SiO_2, hexane/Et_2O). *c*) $Cl_2P(O)F$, Et_3N, CH_2Cl_2, $< 0°$. *d*) CC (SiO_2, hexane/AcOEt).

13 and **14** (see *Exper. Part*) exhibited the same essential features as the type-**I** [1], type-**II** [2], and type-**IV** [3] congeners (*Scheme 1*). In particular, the ^{31}P-NMR spectra confirmed the relative configuration at the P-atom, the double-chair conformations of the axial epimers **13a** and **14a**, and distorted conformations of the 2,4-dioxa-3-phospha moiety in the equatorial epimers **13b** and **14b**[10]). Due to the strongly electronegative F-

[10]) Generally, the ^{31}P-NMR resonance of the axial epimer is shifted upfield with respect to the equatorial one, and the chemical-shift difference ($\Delta\delta = \delta_{eq} - \delta_{ax}$) is > 0, and its magnitude is inversely proportional to the electronegativity of the substituent at the P-atom. However, the cyclic phosphorofluoridates of the *cis*-series of the type **I**–**IV** compounds (*Scheme 1*, L = F) displayed $\Delta\delta < 0$, a fact that is only explained by significant conformational changes. The magnitude of the ^3J(P,H) in the ^{1}H-coupled ^{31}P-NMR is indicative of the conformation of the 2,4-dioxa-3-phospha moiety: Diagnostically relevant values for the axial epimers were $^3J(P,H_{eq}–C(5)) \approx 25$ Hz and $^3J(P,H_{ax}–C(5)) \approx 0$, whereas the equatorial ones displayed $^3J(P,H_{ax}–C(5)) \approx {}^3J(P,H_{eq}–C(5)) \approx 10$–15 Hz. Hence, the axial epimers exhibited a *d*-type and the equatorial ones a *m*-type splitting pattern (see [13]).

substituent, the chemical shift difference ($\Delta\delta = \delta_{eq} - \delta_{ax}$) was small in the *trans*-couple **13a**/**13b** ($\Delta\delta = +0.9$ ppm) and negative in the *cis*-couple **14a**/**14b** ($\Delta\delta = -0.3$ ppm) as discussed earlier [18].

3.2. *Conformations of* **13** *and* **14** *in Solution.* As previously presented [1][2][6–8] and directly evidenced [18], stereoelectronic (anomeric) effects predominantly determine the conformation of the 3-substituted 2,4-dioxa-3-phosphadecalin 3-oxides. In the 3-axially substituted 3-fluoro-3-phosphadecalins **13a** and **14a**, both the steric and the stereoelectronic effects act in the same direction. According to the vicinal couplings ($^3J(P,H_{eq}–C(5)) = 25.3$ Hz (**13a**) and 25.7 Hz, (**14a**))[10], these compounds adopt the double-chair conformation **C-1**[11])[12]) (*Scheme 5*).

Scheme 5

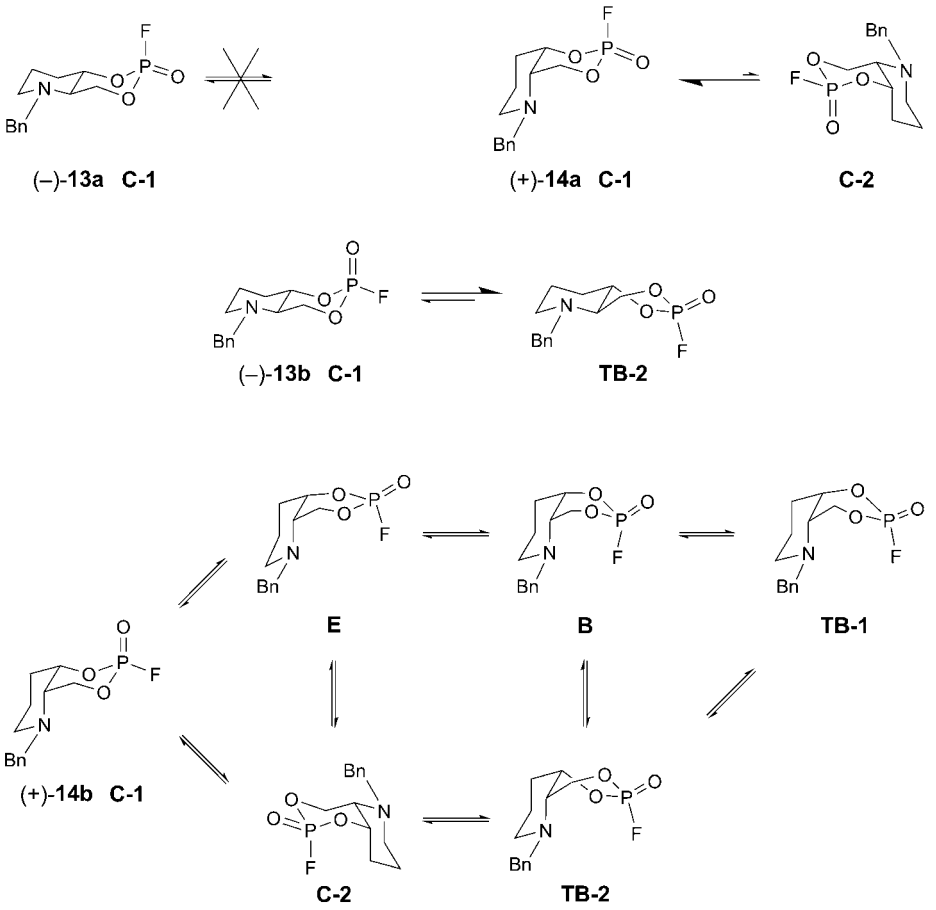

[11]) The short terms for the conformations (IUPAC convention) were introduced in [18]: **C** = chair, **B** = boat, **E** = envelope, **TB** = twist-boat (see also [1][2]).

[12]) There is no evidence for the completely inverted **C-2** conformation in **14a**. We assume that the anomeric preference prevents this interconversion.

Generally, the steric and the stereoelectronic effects are opposite in the *P(3)*-equatorially substituted compounds **13b** and **14b**. Although the chair conformation is sterically favored, the anomeric preference of the F-substituent to move into an axial position results in nonchair conformations such as boat or twist-boats (*i.e.*, **B**, **TB-1**, and **TB-2**)[11]) of the 2,4-dioxa-3-phospha moiety (*Scheme 5*)[13]). Based on our detailed conformational studies on the type-**III** inhibitors [4][18][19], in particular, according to the vicinal coupling data (^3J(P,H$_{ax}$–C(5)) = 14.5, ^3J(P,H$_{eq}$–C(5) = 8.5, and ^3J(P,H–C(1)) ≈ 1 Hz) and the virtual invariability of ^3J(P,H$_{eq}$–C(5)) in low-temperature ^{31}P-NMR experiments [4][18][19], we conclude that the conformation of the *trans*-configured epimers (+)- and (−)-**13b** is an equilibrium mixture of **TB-2** (predominant) and **C-1** (*Scheme 5*)[14]).

In the *cis*-configured equatorial epimers (+)- and (−)-**14b**, the flexibility of the decalin system combined with the anomeric preference of the *P(3)*-equatorial F-substituent render the situation significantly more complex, and additional conformations must be envisaged. In particular, the bicyclic system can undergo complete ring inversion to yield the prominent **C-2** arrangement (*Scheme 5*), which seems to be favored by both the anomeric and the steric effects. According to crystal structures (see [18], and *Figs. 2* and *3*), the piperidine moiety adopts the chair conformation with the *N*-benzyl group in the equatorial position. Although its steric impact is not reliably predictable, it certainly affects the equilibrium population of the conformers, and it would interfere with a complete ring inversion to **C-2**. The diagnostically relevant ^3J(P,H–C(1)) = 12.8, ^3J(P,H$_{ax}$–C(5)) = 14.0, and ^3J(P,H$_{eq}$–C(5)) = 10.9 Hz (see *Exper. Part*) and the interpretation of our modified *Karplus* equation [18] clearly evidenced that the vicinal couplings are averaged, and none of the conformations depicted in *Scheme 5* can be excluded, nor any can be prominently assigned[15]). Hence, **14b** is in solution a complex mixture of the coexisting conformers **C-1**/**C-2**, and/or **TB-1**/**TB-2**, and also **B** and envelope **E**.

A full account of our detailed conformational studies by variable temperature ^{31}P-NMR experiments and X-ray analyses on the 3-fluoro-2,4-dioxa-3-phosphadecalin 3-oxides (type **IV**) and the 7-benzyl-3-fluoro-2,4-dioxa-7-aza congeners (type **III**) will be presented in a following report [19].

3.3. *Crystallographic Analyses of* (−)-**13a** and (+)-**14a**[16]). The structures of (−)-**13a** and (+)-**14a** were solved and refined successfully. Both compounds in the crystal were

---

[13]) In such systems, the resulting minimum-energy conformations represent a balance between the anomeric effect favoring the axial orientation in the twist-boat and the 1,3-steric and eclipsing interactions favoring the chair conformation. This fact explains the unusual stabilization of nonchair conformations.

[14]) Since ^3J(P,H–C(1)) ≈ 1, conformations **B** and **TB-1** are excluded. At room temperature, the ^{31}P-NMR spectra were well resolved and coalescence phenomena were not observed, *i.e.*, the interconversion **C-1** ⇌ **TB-2** is fast on the NMR time scale. By lowering the temperature, **13b** tends to adopt the thermodynamically significantly stabilized **TB-2** conformation, *i.e.*, at sufficiently low temperatures, **TB-2** will freeze out.

[15]) The most striking argument for the exclusion of a prominent conformation is that none of the ^3J(P,H) ≈ 0 [18].

[16]) The full data sets are summarized in *Table 2* (see *Exper. Part*). CCDC-857940 ((−)-**13a**) and CCDC-857941 ((+)-**14a**) contain supplementary crystallographic data. These can be obtained free of charge from the *Cambridge Crystallographic Data Centre via* www.code.cam.ac.uk/data_request/cif.

enantiomerically pure, and the absolute configurations of the molecules were determined independently by the diffraction experiments. The refinement of the absolute structure parameter confidently confirmed that the refined coordinates (*Table 2*, see *Exper. Part*) represent the true enantiomorphs with the expected (1*S*,3*S*,6*R*)-configuration for (−)-**13a** (*Fig. 2*), and the (1*S*,3*S*,6*S*)-configuration for (+)-**14a** (*Fig. 3*). These results independently corroborated the configurational assignments of the precursors (−)-(2*R*,3*S*)-1-benzyl-3-hydroxypiperidine-2-methanol ((−)-**4**) and (−)-(2*S*,3*S*)-1-benzyl-3-hydroxypiperidine-2-methanol ((+)-**5**) by means of the high-field ^{1}H-NMR *Mosher* method and our unusual extension to bis-MTPA derivatives [11]. As discussed above, the six-membered ring containing the P-atom has an undistorted chair conformation with the F-atom in the axial position, and the *N*-benzyl group occupies the sterically favored equatorial position.

Since all attempts to obtain suitable crystals of the equatorial epimers (+)- or (−)-**13b** and/or (+)- or (−)-**14b** were not successful, no X-ray crystallographic analysis of an optically active equatorial type-**III** compound is available[17]).

4. Enzyme Kinetics. – 4.1. *General*. The inhibitory potency and the mode of action of the enantiomerically pure 3-fluoro-7-aza-3-phosphadecalins **13** and **14** was

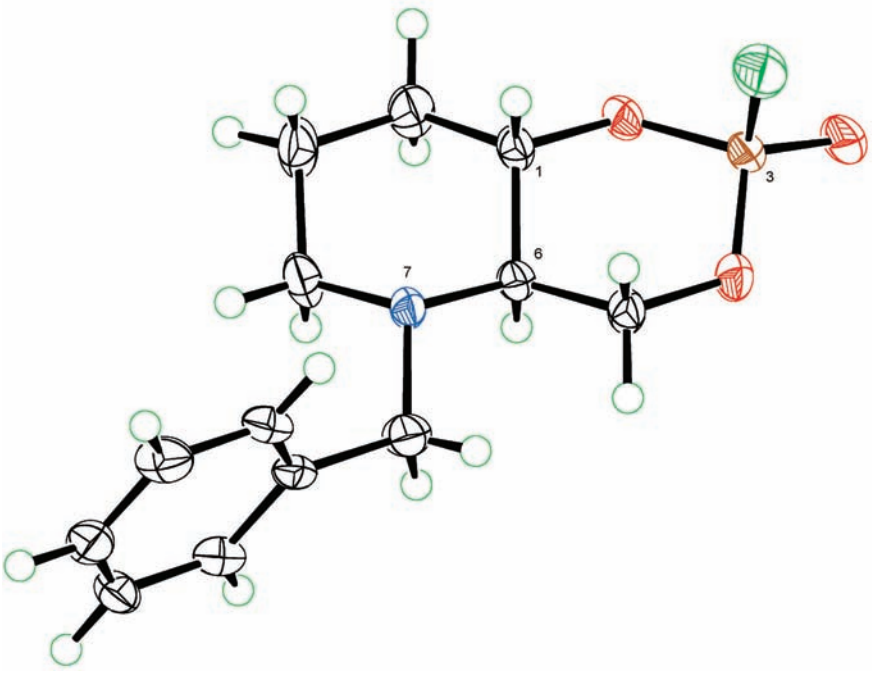

Fig. 2. *Molecular Structure of (−)*-**13a** ((1*S*,3*S*,6*R*)). Trivial atom numbering; 50% probability ellipsoids.

[17]) In contrast to this finding, the racemic equatorial epimers (±)-**13b** and (±)-**14b** could be suitably crystallized [9], and their X-ray crystallographic analyses provided the direct evidence of the anomeric effect [18].

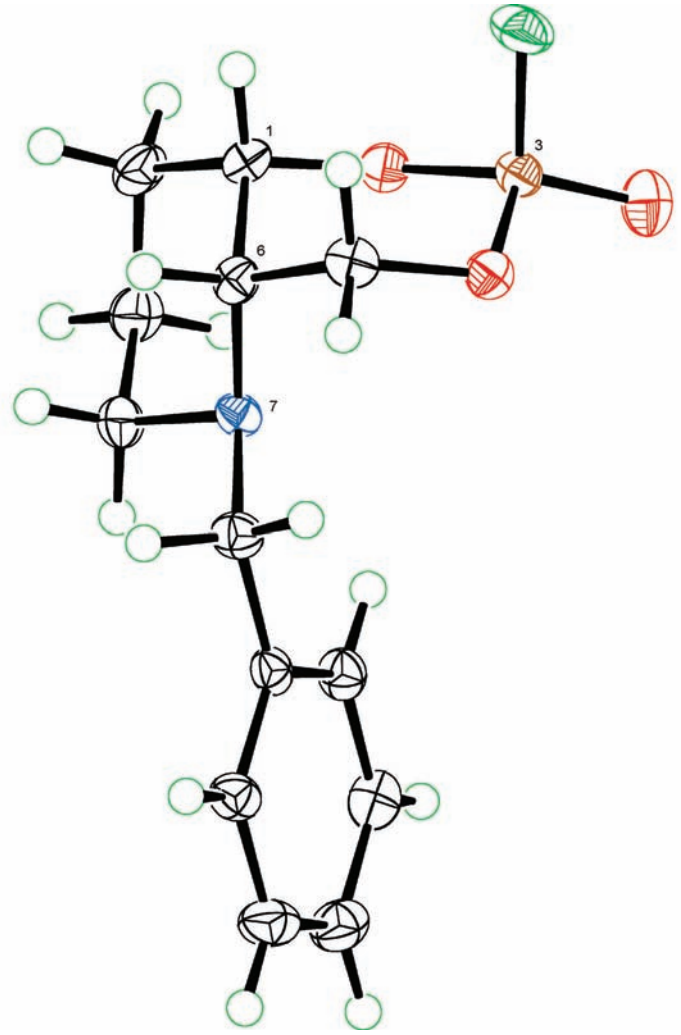

Fig. 3. *Molecular Structure of (+)*-**14a** ((1*S*,3*S*,6*S*)). Trivial atom numbering; 50% probability ellipsoids.

determined according to the general considerations and procedure explicitely described in the precedent reports [1][2]. In particular, the data acquisition was based on the *Ellman* assay [20], and the mathematical evaluation was performed according to [21]. For irreversible inhibition, the simplified overall processes were considered that directly yield the covalently phosphorylated enzyme $\boldsymbol{E}-\boldsymbol{I}$ (*Scheme 6*, mechanism *a*) or involve a preceding reversible step, resulting in the formation of an associative enzyme–inhibitor complex $\boldsymbol{E}\cdot\boldsymbol{I}$*, followed by the irreversible phosphorylation step (*Scheme 6*, mechanism *b*) [1][2].

4.2. *Data Analysis and Results.* The determination of the apparent rate constants (k_{obs}) from the progress curves ($A = f(t)$, see *Eqn. 1* in the *Exper. Part*) and the mathematical evaluation of the dependence $k_{obs} = f([\boldsymbol{I}])$ to evaluate the irreversible

Scheme 6

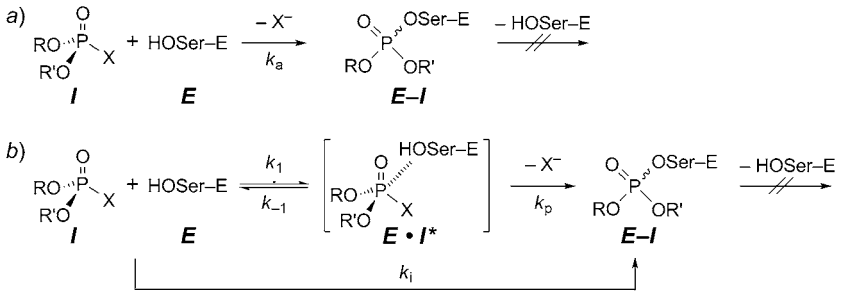

E = Free enzyme: serine hydrolase (acetylcholinesterase, chymotrypsin)
k_1, k_{-1}: Rate constants (also referred to as k_{on} and k_{off}, resp.)
$k_{-1}/k_1 = K_D$: Dissociation constant (also referred to as K_i)
k_a: Association constant
k_p: Phosphorylation constant
$k_i = k_p/K_D$: Overall inhibitory potency ('bimolecular reaction constant')

inhibition parameters (K_D, k_a, k_i, and k_p, resp.) were performed according to [21][18]). The mathematical equations (*Eqns. 1–3*) underlying *Scheme 6* and further details are summarized in the *Exper. Part*. For all the *P(3)*-axially substituted 3-fluoro-7-aza-3-phosphadecalins ((±)-**13a**, (+)- and (−)-**13a**, and (+)- and (−)-**14a**), the secondary plot ($k_{obs} = f([\boldsymbol{I}])$) exhibited a linear dependence, and inhibition mechanism *a* was assigned to these compounds. In the case of (+)- and (−)-**13b** and (+)- and (−)-**14b**, the secondary plot depended hyperbolically upon [***I***], and mechanism *b* was assigned to the the *P(3)*-equatorially substituted congeners. The experimental results are summarized in *Table 1*.

All the investigated 3-fluoro-7-aza-3-phosphadecalins (type **III**) inhibited AChE irreversibly. Compared to diisopropyl phosphorofluoridate ($P(O)F(O^iPr)_2$) that was used as the standard reference, they were moderate inhibitors. But with respect to the related 9-aza- (type **I**) [1] and 8-aza-3-phosphadecalins (type **II**) [2], they were significantly stronger. With the exception of (+)- und (−)-**14a** that did not differ in the inhibition behavior, the type-**III** compounds displayed pronounced diastereoselectivity, the (3*R*)-configured isomers being roughly twice as potent than the *P(3)*-epimers. Furthermore, the data of **13** again confirmed our finding that the inhibitory activity of a racemic inhibitor is approximately the arithmetic mean of the enantiomers [4][19]).

---

[18]) Recently, we have presented a novel, integrated approach with a reappraisal of kinetic mechanisms and diagnostic methods that enables distinct as well as subtle differentiations of generalized inhihibition mechanisms [22]. Although the assay data of the (+)- and (−)-7-benzyl-3-fluoro-2,4-dioxa-7-aza-3-phosphadecalin 3-oxides **13** and **14** were evaluated by the novel method, too [4], we present the results of the simplified procedure [20] for reasons of conformity and direct comparison with the preceding reports in this series [1][2].

[19]) Although apparently obvious, it cannot be concluded *a priori* that the inhibition constants are simply additive.

Table 1. *Kinetic Data of the Inhibition of AChE with the Enantiomerically Pure 7-Aza-3-fluoro-2,4-dioxa-3-phosphadecalins (+)- and (−)-***13** *and (+)- and (−)-***14**. $P(O)F(O^iPr)_2$ as reference.

	Kinetic Parameters	Mechanism[a])		Kinetic Parameters	Mechanism[a])
(+)-**13a**	$k_a = 11.7 \pm 0.4$ м$^{-1}$s^{-1}	*a*	(+)-**14a**	$k_a = 5.1 \pm 0.2$ м$^{-1}$s^{-1}	*a*
(−)-**13a**	$k_a = 6.0 \pm 0.2$ м$^{-1}$s^{-1}	*a*	(−)-**14a**	$k_a = 5.1 \pm 0.3$ м$^{-1}$s^{-1}	*a*
(±)-**13a**	$k_a = 8.6 \pm 0.2$ м$^{-1}$s^{-1}	*a*	(+)-**14b**	$k_i = 123.3 \pm 3.3$ м$^{-1}$s^{-1}	*b*
(+)-**13b**	$k_i = 56.7 \pm 1.2$ м$^{-1}$s^{-1}	*b*		$K_D = 100 \pm 5$ μм	
	$K_D = 103 \pm 2$ μм			$k_p = 0.0075 \pm 0.0001$ s^{-1}	
	$k_p = 0.0059 \pm 0.0002$ s^{-1}		(−)-**14b**	$k_i = 48.3 \pm 0.5$ м$^{-1}$s^{-1}	*b*
(−)-**13b**	$k_i = 105.0 \pm 2.3$ м$^{-1}$s^{-1}	*b*		$K_D = 57 \pm 2$ μм	
	$K_D = 97 \pm 2$ μм			$k_p = 0.070 \pm 0.002$ s^{-1}	
	$k_p = 0.010 \pm 0.001$ s^{-1}		$P(O)F(O^iPr)_2$	$k_a = 245.0 \pm 7.3$ м$^{-1}$s^{-1}	*a*

[a]) see *Scheme 6*.

5. Remarks. – Besides the main object of our research project, the investigation of the stereochemical course of the inhibition reaction by ^{31}P-NMR spectroscopy [4][6–8], kinetic studies are a valuable tool to study molecular interactions of acetylcholine (ACh) with AChE. Being mimetics of rotamers of ACh, the 7-benzyl-3-fluoro-2,4-dioxa-8-aza-3-phosphadecalin 3-oxides **13** and **14** (type-**III** inhibitors) are supposed to be suitable probes to impart knowledge on the physiologically active (recognition) conformation of ACh in the course of the hydrolysis. This enzymatic process is a nearly diffusion controlled, highly complex reaction cascade where all steps are governed by conformational changes of both the enzyme and the substrate[20]). Meanwhile, we have evaluated the kinetic data of the 3-fluoro substituted 2,4-dioxa-3-phosphadecalins of the types **I**–**IV** (*Scheme 1*), but our experimental results still do not allow reliable conclusions with respect to the effective inhibition mechanism (active site, peripheral or other conformatively induced irreversible binding at another nucleophilic site). Considering the fact that our compounds differ from the natural substrate and have additional structural features that significantly could influence both the steric demand and the basicity of the compound, the situation is even more complicated, and conclusions of evidencing a recognition conformation from the inhibitory data would remain rather speculative. However, it is not clear to what extent this fact is due to the simplified kinetic approach (see *Scheme 6*) and the respective mathematical treatment [21]. A complete re-interpretation of the kinetic data of the types **I**–**IV** according to our integrated approach [22][18]) and the full comparison of the respective data sets and their interpretation is in process and will be presented in a following, concluding report [23].

The authors are indebted to PD Dr. *A. Linden*, head of the X-ray department of our institute for the high-quality X-ray crystallographic analyses. The financial support of the project by the *Swiss National Science Foundation* is gratefully acknowledged.

[20]) For a brief discussion of the recognition conformation of ACh, see [1].

Experimental Part

1. *General.* See [1][7][9]. For the particular precautions in preparing and handling the organophosphates, see [9]. Determination of ee: based on the integration of the peak areas of the anal. HPLC separations of the precursor diols with optimized resolution ($R_s > 4$). NMR Assignments: based on extensive 2D-NMR (see [9]) and selective ^{1}H-decoupling experiments.

2. *(+)-(2S,3R)- and (−)-(2R,3S)-, and (+)-(2S,3S)- and (−)-(2R,3R)-3-Hydroxy-1-(phenylmethyl)-piperidine-2-methanol* ((+)- and (−)-**4**, and (+)- and (−)-**5**, resp.). 2.1. *[3-(Acetyloxy)-1-(phenylmethyl)piperidin-2-yl]methyl 2,2-Dimethylpropanoates* **2** *and* **3**. The racemic precursors, the (±)-*trans*- and (±)-*cis*-diesters (±)-**2** and (±)-**3**, resp., were prepared and characterized as described earlier [9]. Prep. HPLC of (±)-**2** (*Chiralcel® OD*, hexane/(±)-2-BuOH 200:1; $\alpha = 1.24$, $R_S = 4.95$) afforded enantiomerically pure (+)-**2** ($k' = 1.68$) and (−)-**2** ($k' = 2.08$) as yellowish crystals. Prep. HPLC of (±)-**3** (*Chiralcel® OD*, hexane/^{i}PrOH 100:1; $\alpha = 1.36$, $R_S = 6.4$) furnished enantiomerically pure (+)-**3** ($k' = 0.74$) and (−)-**3** ($k' = 1.01$) as yellowish viscous oils. Colorless products were obtained by subjecting (+)- and (−)-**2** and (+)- and (−)-**3** to CC (SiO_2, (hexane/AcOEt 4:1).

(+)-(2S,3R)-[3-(Acetyloxy)-1-(phenylmethyl)piperidin-2-yl]methyl 2,2-Dimethylpropanoate ((+)-**2**)[21]): Colorless crystals. M.p. 44–46°. R_f (hexane/AcOEt 4:1) 0.25. $[\alpha]_D^{25} = +12.4$ ($c = 1.15$, EtOH, ee > 99%).

(−)-(2R,3S)-[3-(Acetyloxy)-1-(phenylmethyl)piperidin-2-yl]methyl 2,2-Dimethylpropanoate ((−)-**2**): $[\alpha]_D^{25} = -12.2$ ($c = 1.11$, EtOH, ee > 99%). All other data identical with those of (+)-**2**.

(+)-(2R,3R)-[3-(Acetyloxy)-1-(phenylmethyl)piperidin-2-yl]methyl 2,2-Dimethylpropanoate ((+)-**3**)[21]): Colorless viscous oil. R_f (hexane/AcOEt 4:1) 0.20. $[\alpha]_D^{25} = +9.1$ ($c = 1.10$, EtOH, ee > 99%).

(−)-(2S,3S)-[3-(Acetyloxy)-1-(phenylmethyl)piperidin-2-yl]methyl 2,2-Dimethylpropanoate ((−)-**3**): $[\alpha]_D^{25} = -9.0$ ($c = 1.28$, EtOH, ee > 99%). All other data identical with those of (+)-**3**.

2.2. *3-Hydroxy-1-(phenylmethyl)piperidine-2-methanols* **4** *and* **5**. Saponification of the diester (+)- or (−)-**2** or (+)- or (−)-**3** (each 500 mg, 1.44 mmol) in EtOH (10 ml) with KOH (600 mg) in H_2O (15 ml) at r.t. (3 h) and usual workup afforded the crude diol (+)- or (−)-**4**, or (−)- or (+)-**5**, resp., as yellowish viscous oils. After boiling in EtOH over charcoal, the pure compounds were obtained as colorless crystals (310–318 mg, 97–100%).

(+)-(2S,3R)-3-Hydroxy-1-(phenylmethyl)piperidine-2-methanol ((+)-**4**[22]): Colorless prisms. M.p. 81–84°. R_f (AcOEt) *ca.* 0.20 (tailing). $[\alpha]_D^{25} = +43.5$ ($c = 1.05$, EtOH, ee > 99%).

(−)-(2R,3S)-3-Hydroxy-1-(phenylmethyl)piperidine-2-methanol ((−)-**4**): $[\alpha]_D^{25} = -43.7$ ($c = 1.08$, EtOH, ee > 99%). All other data identical with those of (+)-**4**.

(+)-(2S,3S)-3-Hydroxy-1-(phenylmethyl)piperidine-2-methanol ((+)-**5**[22]): Colorless prisms. M.p. 75–77°. R_f (AcOEt) *ca.* 0.18 (tailing). $[\alpha]_D^{25} = +21.3$ ($c = 1.02$, EtOH, ee > 99%).

(−)-(2R,3R)-3-Hydroxy-1-(phenylmethyl)piperidine-2-methanol ((−)-**5**): $[\alpha]_D^{25} = -21.5$ ($c = 0.55$, EtOH, ee > 99%). All other data identical with those of (+)-**5**.

3. *(R)- and (S)-MTPA Derivatives for the Determination of the Absolute Configuration.* 3.1. *Bis-MTPA Esters* **6a**, **6b**, **7a**, **7b**, **8a**, **8b**, **9a**, *and* **9b**. Each diol (±)- or (+)-**4**, or (−)- or (+)-**5** (each 17.5 mg, 0.08 mmol) was dissolved in anh. CH_2Cl_2 (3 ml), and Et_3N (46 µl, 0.32 mmol) and *N*,*N*-dimethylpyridin-4-amine (DMAP; 2 mg) were added under Ar. The mixture was treated with (+)-(*S*)-MTPA-Cl (34 µl, 0.18 mmol). After stirring for 1 h at r.t. under Ar, the mixture was subjected to CC (SiO_2, hexane/Et_2O 1:9): (*R*)-MTPA diester **6a**, **7a**, **8a**, or **9a**. Analogously, (−)- or (+)-**4**, or (−)- or (+)-**5** was treated with (−)-(*R*)-MTPA-Cl to yield the (*S*)-MTPA diester **6b**, **7b**, **8b**, or **9b**. All MTPA derivatives were isolated in pure form as colorless, viscous oils: **6a** (47 mg, 90%), **6b** (48 mg, 92%), **7a** (49 mg, 94%), **7b** (48 mg, 92%), **8a** (50 mg, 95%), **8b** (51 mg, 98%), **9a** (48 mg, 92%), and **9b** (50 mg, 95%).

(2S,3R)-1-(Phenylmethyl)-2-{[(2R)-3,3,3-trifluoro-2-methoxy-1-oxo-2-phenylpropoxy]methyl}piperidin-3-yl (αR)-α-Methoxy-α-(trifluoromethyl)benzeneacetate (Bis-(*R*)-MTPA ester; **7a**) *from (+)-***4**: R_f (AcOEt) 0.69. ^{1}H-NMR (500 MHz, $CDCl_3$): 7.56–7.50 (*m*, 4 arom. H); 7.42–7.33 (*m*, 6 arom. H); 7.26–7.12 (*m*, 5 arom. H); 5.05 (*M* of *ABXM*, *ddd*, $^3J(3,2) = 6.8$, $^3J(3,4ax) = 7.6$, $^3J(3,4eq) = 4.2$,

[21]) The spectral data were identical with those of (±)-**2** and (±)-**3**, resp., see [9].

[22]) The spectral data were identical with those of (±)-**4** and (±)-**5**, resp., see [9].

H–C(3)); 4.65, 4.46 (*AB* of *ABXM*, ^2J = 12.2, ^3J = 4.3, 3.8, CH_2(OMTPA)); 3.89, 3.32 (*AB*, ^2J = 13.2, PhCH_2); 3.54, 3.51 (2*q*, ^5J(Me,F) = 1.1, MeO); 2.85 (*X* of *ABXM*, ^3J(2,3) = 6.8, ^3J(2,CH$_2$) = 4.3, 3.8, H–C(2)); 2.63 (*ddd*, ^2J = 10.5, ^3J(6eq,5eq) = 6.6, ^3J(6eq,5ax) = 3.5, H$_{eq}$–C(6)); 2.13 (*ddd*, ^2J = 11.8, ^3J(6ax,5ax) = 8.2, ^3J(6ax,5eq) = 3.3, H$_{ax}$–C(6)); 2.05 (*ddt*, ^2J = 11.3, ^3J(4eq,3) = ^3J(4eq,5ax) = 4.2, ^3J(4eq,5eq) = 8.0, H$_{eq}$–C(4)); 1.60 (*m*, $w_{1/2} \approx 15$, H$_{eq}$–C(5)); 1.51 (*m*, $w_{1/2} \approx 20$, H$_{ax}$–C(4)); 1.41 (*m*, $w_{1/2} \approx 20$, H$_{ax}$–C(5)). ^{13}C-NMR (75 MHz, CDCl$_3$): 166.6, 165.7 (CO of MTPA); 138.5 (C(1′)), 132.1, 132.0 (C(1″), C(1‴)); 129.7 (C(4″), C(4‴)); 129.6 (C(2′), C(6′)); 128.5 (C(2″), C(2‴), C(6″), C(6‴)); 128.2 (C(3′), C(5′)); 127.4 (C(3″), C(3‴), C(5″), C(5‴)); 127.3 (C(4′)); 123.4, 123.3 (2*q*, ^1J(C,F) = 289, CF$_3$); 84.8, 84.7 (2*q*, ^2J(C,F) = 27.8, Ph*C*(OMe)(CF$_3$)CO); 72.3 (C(3)); 62.1 (C(2)); 61.6 (Ph*C*H$_2$); 57.9 (C(8)); 55.5, 55.3 (MeO); 48.8 (C(6)); 27.4 (C(4)); 20.9 (C(3)). ^{19}F{^{1}H}-NMR (376.5 MHz, CDCl$_3$): −70.46, −71.65 (2*s*, CF$_3$).

*(2S,3*R*)-1-(Phenylmethyl)-2-{[(2*S*)-3,3,3-trifluoro-2-methoxy-1-oxo-2-phenylpropoxy]methyl}piperidin-3-yl (α*S*)-α-Methoxy-α-(trifluoromethyl)benzeneacetate* (Bis-(*S*)-MTPA ester; **7b**) *from (+)-***4**: R_f (AcOEt): 0.69. ^{1}H-NMR (500 MHz, CDCl$_3$): 7.60–7.47 (*m*, 4 arom. H); 7.40–7.31 (*m*, 6 arom. H); 7.26–7.18 (*m*, 3 arom. H); 7.16–7.12 (*m*, 2 arom. H); 5.05 (*M* of *ABXM*, *td*, ^3J(3,2) = ^3J(3,4ax) = 8.3, ^3J(3,4eq) = 4.2, H–C(3)); 4.70, 4.05 (*AB* of *ABXM*, ^2J = 12.3, ^3J = 3.2, 3.0, CH_2(OMTPA)); 3.98, 3.17 (*AB*, ^2J = 13.4, PhCH_2); 3.55 (br. *s*, 2 MeO); 2.72 (*m*, br. *q*-like, $w_{1/2} \approx 18$, H$_{eq}$–C(6)); 2.69 (*X* of *ABXM*, not resolved, H–C(2)); 2.20 (*m*, *td*-like, $w_{1/2} \approx 20$, H$_{eq}$–C(4)); 2.03 (*m*, *td*-like, $w_{1/2} \approx 25$, H$_{ax}$–C(6)); 1.64 (*qd*-like, $w_{1/2} \approx 18$, H$_{eq}$–C(5)); 1.56–1.41 (*m*, H$_{ax}$–C(4), H$_{ax}$–C(5)). ^{13}C-NMR (75 MHz, CDCl$_3$): 166.4, 165.4 (CO of MTPA); 138.4 (C(1′)), 132.5, 132.2 (C(1″), C(1‴)); 129.7 (C(4″), C(4‴)); 128.7 (C(2′), C(6′)); 128.5 (C(2″), C(2‴), C(6″), C(6‴)); 128.3 (C(3′), C(5′)); 127.4 (C(3″), C(3‴), C(5″), C(5‴)); 127.1 (C(4′)); 123.4 (*q*, ^1J(C,F) = 289, CF$_3$); 84.8, 84.4 (2*q*, ^2J(C,F) = 27.8, Ph*C*(OMe)(CF$_3$)CO); 72.3 (C(3)); 63.1 (C(2)); 61.6 (Ph*C*H$_2$); 57.9 (C(8)); 55.6, 55.2 (MeO); 50.1 (C(6)); 28.7 (C(4)); 22.7 (C(3)). ^{19}F{^{1}H}-NMR (376.5 MHz, CDCl$_3$): −71.52, −71.58 (2*s*, CF$_3$)).

$\Delta\delta(^1H) = \delta(S) - \delta(R)$ (in Hz): H–C(2), −80; H–C(3), 0; H$_{ax}$–C(4), −10; H$_{eq}$–C(4), +75; H$_{ax}$–C(5), +35; H$_{eq}$–C(5), +20, H$_{ax}$–C(6), −50; H$_{eq}$–C(6), +45 → (3*R*)-configuration.

*(*R*)- and (*S*)-MTPA Esters* **6a** *and* **6b** *from* (−)-**4**. Being enantiomeric compounds, **6a** and **7b** (**6a** = *ent*-**7b**), as well as **6b** and **7a** (**6b** = *ent*-**7a**), exhibited identical NMR spectra, only the sign of $\Delta\delta$ was inverted: $\Delta\delta(^1H) = \delta(S) - \delta(R)$ (in Hz): H–C(2), +80; H–C(3), 0; H$_{ax}$–C(4), +10; H$_{eq}$–C(4), −75; H$_{ax}$–C(5), −35; H$_{eq}$–C(5), −20; H$_{ax}$–C(6), +50, H$_{eq}$–C(6), −45 → (3*S*)-configuration.

*(2S,3*S*)-1-(Phenylmethyl)-2-{[(2*R*)-3,3,3-trifluoro-2-methoxy-1-oxo-2-phenylpropoxy]methyl}piperidin-3-yl (α*R*)-α-Methoxy-α-(trifluoromethyl)benzeneacetate* (Bis-(*R*)-MTPA ester; **9a**) *from (+)-***5**: R_f (AcOEt): 0.70. ^{1}H-NMR (500 MHz, CDCl$_3$): 7.55–7.48 (*m*, 4 arom. H); 7.41–7.36 (*m*, 6 arom. H); 7.28–7.18 (*m*, 5 arom. H); 5.30 (*M* of *ABXM*, *dt*, ^3J(3,2) = ^3J(3,4eq) = 4.0, ^3J(3,4ax) = 7.8, H–C(3)); 4.49, 4.22 (*AB* of *ABXM*, ^2J = 11.8, ^3J = 6.4, 4.2, CH_2(OMTPA)); 3.65, 3.42 (*AB*, ^2J = 14.0, PhCH_2); 3.54, 3.48 (2*q*, ^5J(Me,F) = 1.1, MeO); 3.17 (*X* of *ABXM*, ^3J(2,3) = 4.0, ^3J(2,CH$_2$) = 6.4, 4.2, H–C(2)); 2.56 (*ddd*, ^2J = 11.5, ^3J(6eq,5eq) = 7.7, ^3J(6eq,5ax) = 3.6, H$_{eq}$–C(6)); 2.31 (*ddd*, ^2J = 11.5, ^3J(6ax,5ax) = 7.1, ^3J(6ax,5eq) = 4.0, H$_{ax}$–C(6)); 1.80 (*m*, $w_{1/2} \approx 20$, CH$_2$(4)); 1.58 (*m*, $w_{1/2} \approx 70$, CH$_2$(5)). ^{13}C-NMR (75 MHz, CDCl$_3$): 166.3, 165.7 (CO of MTPA); 139.0 (C(1′)); 132.3, 132.0 (C(1″), C(1‴)); 129.7 (C(4″), C(4‴)); 128.5 (C(2′), C(6′)); 128.2 (C(2″), C(2‴), C(6‴), C(6″)); 128.1 (C(3′), C(5′)); 127.3, 127.2 (C(3″), C(3‴), C(5″), C(5‴)); 127.0 (C(4′)); 123.4, 123.3 (2*q*, ^1J(C,F) = 289, CF$_3$); 84.8, 84.7 (2*q*, ^2J(C,F) = 27.8, Ph*C*(OMe)(CF$_3$)CO); 72.8 (C(3)); 63.2 (C(2)); 60.7 (Ph*C*H$_2$); 57.9 (C(8)); 55.4 (MeO); 47.5 (C(6)); 27.1 (C(4)); 21.1 (C(3)). ^{19}F{^{1}H}-NMR (376.5 MHz, CDCl$_3$): −71.45, −71.46 (2*s*, CF$_3$).

*(2S,3*S*)-1-(Phenylmethyl)-2-{[(2*S*)-3,3,3-trifluoro-2-methoxy-1-oxo-2-phenylpropoxy]methyl}piperidin-3-yl (α*S*)-α-Methoxy-α-(trifluoromethyl)benzeneacetate* (Bis-(*S*)-MTPA ester; **9b**) *from (+)-***5**: R_f (AcOEt): 0.70. ^{1}H-NMR (500 MHz, CDCl$_3$): 7.54–7.47 (*m*, 4 arom. H); 7.41–7.34 (*m*, 6 arom. H); 7.28–7.15 (*m*, 5 arom. H); 5.23 (*M* of *ABXM*, *dt*, ^3J(3,2) = ^3J(3,4eq) = 4.0, ^3J(3,4ax) = 7.6, H–C(3)); 4.66, 4.23 (*AB* of *ABXM*, ^2J = 11.7, ^3J = 6.5, 4.6, CH_2(OMTPA)); 3.58, 3.43 (*AB*, ^2J = 14.1, PhCH_2); 3.50, 3.49 (2*q*, ^5J(Me,F) = 0.9, MeO); 3.21 (*X* of *ABXM*, ^3J(2,3) = 4.0, ^3J(2,CH$_2$) = 6.5, 4.6, H–C(2)); 2.56 (*ddd*, ^2J = 11.9, ^3J(6eq,5eq) = 7.6, ^3J(6eq,5ax) = 3.3, H$_{eq}$–C(6)); 2.32 (*ddd*, ^2J = 11.9, ^3J(6ax,5ax) = 6.6, ^3J(6ax,5eq) = 3.8, H$_{ax}$–C(6)); 1.71 (*m*, $w_{1/2} \approx 25$, CH$_2$(4)); 1.52 (*m*, $w_{1/2} \approx 70$, CH$_2$(5)). ^{13}C-NMR (75 MHz, CDCl$_3$): 166.4, 165.8 (CO of MTPA); 139.1 (C(1′)); 132.1, 132.0 (C(1″), C(1‴)); 129.7 (C(4″), C(4‴)); 128.5 (C(2′), C(6′)); 128.2 (C(2″), C(2‴), C(6″), C(6‴)); 128.1 (C(3′), C(5′)); 127.4, 127.2

(C(3″), C(3‴), C(5″), C(5‴)); 126.9 (C(4′)); 123.4, 123.3 (2*q*, ^1J(C,F) = 289, CF_3); 84.7, 84.6 (2*q*, ^2J(C,F) = 27.8, Ph*C*(OMe)(CF_3)CO); 72.8 (C(3)); 63.0 (C(2)); 60.8 (Ph*C*H$_2$); 57.9 (C(8)); 55.5, 55.3 (MeO); 47.8 (C(6)); 26.8 (C(4)); 21.0 (C(3)). ^{19}F{^{1}H}-NMR (376.5 MHz, $CDCl_3$): −71.48, −71.60 (2*s*, CF_3).

$\Delta\delta(^1H) = \delta(S) - \delta(R)$ (in Hz): H–C(2), +20; H–C(3), −35; H_{ax}–C(4) ≈ H_{eq}–C(4), −45; H_{ax}–C(5) ≈ H_{eq}–C(5), −30; H_{ax}–C(6), +5; H_{eq}–C(6), 0 → (3*S*)-configuration.

*(*R*)- and (*S*)-MTPA Esters* **8a** and **8b** *from* (−)-**5**. Being enantiomeric compounds, **8a** and **9b** (**8a** = *ent*-**9b**) as well as **8b** and **9a** (**8b** = *ent*-**9a**) exhibited identical NMR spectra, only the sign of $\Delta\delta$ was inverted: $\Delta\delta(^1H) = \delta(S) - \delta(R)$ (in Hz): H–C(2), −20; H–C(3), +35; H_{ax}–C(4) ≈ H_{eq}–C(4), +45; H_{ax}–C(5) ≈ H_{eq}–C(5), +30; H_{ax}–C(6), −5; H_{eq}–C(6), 0 → (3*R*)-configuration.

3.2. *[(Pivaloyloxy)methyl]-Substituted MTPA Esters* **11** *and* **12**. The soln. of (±)-**10** (77 mg. 0.25 mmol, prepared according to [9]) in anh. CH_2Cl_2 (5 ml), Et_3N (44 µl, 0.31 mmol), and *N*,*N*-dimethylpyridin-4-amine (DMAP; 2 mg) was treated with (+)-(*S*)-MTPA-Cl (55 µl, 0.30 mmol). After stirring for 2 h at r.t. under Ar, the mixture was subjected to CC (SiO_2, hexane/Et_2O 1:9) to afford the mixture of the diastereoisomeric (*R*)-MTPA esters **11**/**12** (120 mg, 92%). Prep. HPLC (*Chiralcel® OD*, hexane/^{i}PrOH 150:1; $\alpha = 1.16$, $R_S = 1.6$) afforded the diasteroisomers **11** and **12** (de > 90%) as slightly yellowish oils. Saponification (*cf. Sect.* 2.2) of **11** yielded (−)-**5**, and from **12** we obtained (+)-**5** (< 95%).

*(2*R*,3*R*)-1-Benzyl-2-[(2,2-dimethyl-1-oxopropoxy)methyl]piperidin-3-yl (α*R*)-α-Methoxy-α-(trifluoromethyl)benzeneacetate* ((*R*)-MTPA ester; **11**): R_f (AcOEt) 0.67. $k' = 1.19$ (de = 90%). ^{1}H-NMR (400 MHz, $CDCl_3$): 7.51–7.46 (*m*, 2 arom. H); 7.35–7.31 (*m*, 3 arom. H); 7.24–7.13 (*m*, 5 arom. H); 5.26 (*M* of *ABXM*, *dt*, ^3J(3,4ax) = 6.6, ^3J(3,2) = ^3J(3,4eq) = 3.3, H–C(3)); 4.39, 3.92 (*AB* of *ABXM*, ^2J = 11.5, ^3J = 6.3, ^3J = 5.6, C*H*$_2$(OMTPA)); 3.73 3.39 (*AB*, ^2J = 14.1, PhC*H*$_2$); 3.48 (*q*, ^5J(Me,F) = 1.0, MeO); 2.98 (*X* of *ABXM*, ^3J(2,3) = 3.3, ^3J(2,CH$_2$) = 6.3, 5.6, H–C(2)); 2.59 (*ddd*, ^2J = 11.7, ^3J(6eq,5eq) = 6.2, ^3J(6eq,5ax) = 3.8, H_{eq}–C(6)); 2.16 (*ddd*, ^2J = 11.7, ^3J(6ax,5ax) = 8.4, ^3J(6ax,5eq) = 3.5, H_{ax}–C(6)); 1.77 (*m*, $w_{1/2}$ ≈ 18, H_{eq}–C(4)); 1.62 (*m*, $w_{1/2}$ ≈ 22, H_{ax}–C(4)); 1.61–1.33 (*m*, CH_2(5)); 1.12 (*s*, Me_3C). ^{13}C-NMR (100 MHz, $CDCl_3$): 178.0 (*C*OCMe$_3$); 165.9 (CO of MTPA); 139.3 (C(1′)); 132.0 (C(1″)); 129.5 (C(4″)); 128.4 (C(2′), C(6′)); 128.2 (C(2″), C(6″)); 128.1 (C(3′), C(5′)); 127.3, 127.2 (C(3″), C(5″)); 126.8 (C(4′)); 123.3 (*q*, ^1J(C,F) = 289, CF_3); 84.6 (*q*, ^2J(C,F) = 27.6, Ph*C*(OMe)(CF_3)CO); 72.5 (C(3)); 61.8 (C(2)); 61.1 (Ph*C*H$_2$); 58.0 (C(8)); 55.3 (MeO); 49.2 (C(6)); 38.6 (Me_3C); 27.3 (C(4)); 27.1 (*Me*$_3$C); 20.7 (C(5)). ^{19}F{^{1}H}-NMR (376.5 MHz, $CDCl_3$): −71.65 (*s*, CF_3).

*(2*S*,3*S*)-1-Benzyl-2-[(2,2-dimethyl-1-oxopropoxy)methyl]piperidin-3-yl (α*R*)-α-Methoxy-α-(trifluoromethyl)benzeneacetate* ((*R*)-MTPA ester; **12**). R_f (AcOEt) 0.67. $k' = 1.38$ (de = 83%). ^{1}H-NMR (400 MHz, $CDCl_3$): 7.52–7.47 (*m*, 2 arom. H); 7.36–7.30 (*m*, 3 arom. H); 7.25–7.13 (*m*, 5 arom. H); 5.28 (*M* of *ABXM*, *dt*, ^3J(3,4ax) = 6.9, ^3J(3,2) = ^3J(3,4eq) = 3.3, H–C(3)); 4.34, 3.78 (*AB* of *ABXM*, ^2J = 11.6, ^3J = 6.4, ^3J = 5.2, C*H*$_2$(OMTPA)); 3.72, 3.39 (*AB*, ^2J = 14.1, PhC*H*$_2$); 3.51 (*q*, ^5J(Me,F) = 1.0, MeO); 2.97 (*X* of *ABXM*, ^3J(2,3) = 3.3, ^3J(2,CH$_2$) = 6.4, 5.2, H–C(2)); 2.60 (*ddd*, ^2J = 11.6, ^3J(6eq,5eq) = 6.4, ^3J(6eq,5ax) = 3.4, H_{eq}–C(6)); 2.18 (*ddd*, ^2J = 11.6, ^3J(6ax,5ax) = 7.9, ^3J(6ax,5eq) = 3.4, H_{ax}–C(6)); 1.81 (*m*, $w_{1/2}$ ≈ 18, H_{eq}–C(4)); 1.69 (*m*, $w_{1/2}$ ≈ 22, H_{ax}–C(4)); 1.62–1.41 (*m*, CH_2(5)); 1.12 (*s*, Me_3C). ^{13}C-NMR (100 MHz, $CDCl_3$): 178.1 (*C*OCMe$_3$), 165.9 (CO of MTPA); 139.4 (C(1′)); 132.2 (C(1″)); 129.6 (C(4″)); 128.4 (C(2′), C(6′)); 128.2 (C(2″), C(6″)); 128.1 (C(3′), C(5′)); 127.3 (C(3″), C(5″)); 126.9 (C(4′)); 123.4 (*q*, ^1J(C,F) = 289, CF_3); 84.1 (*q*, ^2J(C,F) = 27.8, Ph*C*(OMe)(CF_3)CO); 72.6 (C(3)); 61.5 (C(2)); 61.3 (Ph*C*H$_2$); 58.2 (C(8)); 55.4 (MeO); 48.9 (C(6)); 38.6 (Me_3C); 27.5 (C(4)); 27.1 (*Me*$_3$C); 21.2 (C(5)). ^{19}F{^{1}H}-NMR (376.5 MHz, $CDCl_3$): −71.64 (*s*, CF_3).

$\Delta\delta(^1H) = \delta$(**12**) − δ(**11**) (in Hz): H–C(2), −4; H–C(3), +8; H_{ax}–C(4), +28; H_{eq}–C(4), +16; CH_2(5), +20; H_{ax}–C(6), +8; H_{eq}–C(6), +4 → (2*R*,3*R*)-configuration of **11**, (2*S*,3*S*)-configuration of **12**.

4. trans- *and* cis-*5-Benzyl-2-fluoro-1,3-dioxa-5-aza-2-phosphadecalin 2-Oxides (=2-Fluorohexahydro-5-(phenylmethyl)-4*H*-1,3,2-dioxaphosphorino[5,4-*b*]pyridine 2-Oxides) (+)- and (−)-***13a**, (+)- and (−)-***13b**, (+)- and (−)-***14a**, and (+)- and (−)-***14b**, resp.* To a cooled soln. (< 0°) of (+)-**4** (100 mg, 0.45 mmol) in anh. Et_2O (3 ml) and anh. Et_3N (155 µl, 1.1 mmol) in a glove box under N_2, a cooled soln. (< 0°) of $POCl_2F$ [24] (49 µl, 76.8 mg, 0.56 mmol, 1.2 equiv.) in anh. Et_2O (1 ml) was added with a syringe. The mixture was stirred for 2 min at 0°and then withdrawn and subjected to a fast CC (SiO_2 *60* (15–

40 μm, *Merck* No. *115111*), pH 5.6 [7], Et_2O). The eluate was gently concentrated (N_2 stream, $<30°$), and the residue (+)-**13a**/(+)-**13b** (125 mg; ax/eq *ca.* 1.5 : 1) was subjected to CC (SiO_2, pH 5.6 [7], hexane/Et_2O 1 : 2): (+)-**13a** (62 mg, 49%) and (+)-**13b** (27 mg, 22%). Applying the same procedure, phosphorylation of (−)-**4** (97 mg, 0.44 mmol) afforded (−)-**13a** (70 mg, 57%) and (−)-**13b** (21 mg, 16%); the axial epimers were less polar. Due to pronounced epimerization of (+)- and (−)-**13b** during chromatography, the contact time with SiO_2 had to be minimized (< 10 min). Similarly, the *cis*-configured compounds were obtained after phosphorylation and CC (SiO_2, pH 5.6 [7], hexane/AcOEt 1 : 1): from (+)-**5** (101 mg, 0.46 mmol), (+)-**14a** (50 mg, 39%) and (+)-**14b** (59 mg, 46%); from (−)-**5** (105 mg, 0.47 mmol); (−)-**14a** (48 mg, 36%) and (−)-**14b** (54 mg, 40%); the equatorial epimers were less polar.

*(+)-(1*R*,3*R*,6*S*)-7-Benzyl-3-fluoro-2,4-dioxa-7-aza-3-phosphadecalin 3-Oxide* (*=(+)-(2*R*,4a*S*, 8a*R*)-2-Fluorohexahydro-5-(phenylmethyl)-4*H*-1,3,2-dioxaphosphorino[5,4-*b*]pyridine 2-Oxide*; (+)-**13a**): Colorless prisms. M.p. 82.5–84° ((±)-**13a**: m.p. 116.5–118.5° [9]). R_f (hexane/Et_2O 1 : 2) 0.26. $[\alpha]_D^{25} = +70.7$ ($c = 0.29$, acetone). IR (KBr): identical with that of (±)-**13a** [9]. ^{1}H-NMR (400 MHz, (D_6)acetone): 7.36–7.22 (*m*, *Ph*CH_2); 4.92 (*A* of *ABX-P*, $^2J = 10.8$, ^3J(5eq,P) = 25.3, ^3J(5eq,6) = 4.2, H_{eq}–C(5)); 4.44 (*ddd*, ^3J(1,6) = 10.5, ^3J(1,10ax) = 9.0, ^3J(1,10eq) = 4.8, H–C(1)); 4.35 (*B* of *ABX-P*, $^2J = {}^3J$(5ax,6) = 10.8, ^3J(5ax,P) ≈ 1, H_{ax}–C(5)); 3.96, 3.37 (*AB*, $^2J = 13.8$, PhCH_2); 2.86 (*m*, *d*-like, $w_{1/2} \approx 15$, $^2J \approx 12$, H_{eq}–C(8)); 2.72 (*X* of *ABX-P*, ^3J(6,1) = 10.5, ^3J(6,5ax) = 10.8, ^3J(6,5eq) = 4.2, H–C(6)); 2.18–2.07 (*m*, H_{eq}–C(10)); 2.15 (*td*, $^2J = {}^3J$(8ax,9ax) = 12.0, ^3J(8ax,9eq) = 3.0, H_{ax}–C(8)); 1.73–1.69 (*m*, H_{eq}–C(9)); 1.68–1.55 (*m*, H_{ax}–C(9), H_{ax}–C(10)). ^{13}C-NMR (100 MHz, (D_6)acetone): 139.7 (C(1′)); 129.4 (C(3′), C(5′)); 129.3 (C(2′), C(6′)); 128.1 (C(4′)); 83.2 (*dd*, ^2J(1,P) = 7.2, ^3J(1,F) = 1.8, C(1)); 73.5 (*d*, ^2J(5,P) = 8.0, C(5)); 62.2 (*d*, ^3J(6,P) = 4.8, C(6)); 58.3 (Ph*C*H_2); 53.3 (C(8)); 31.9 (*d*, ^3J(10,P) = 9.5, C(10)); 23.7 (*d*, ^4J(9,P) = 2.4, C(9)). ^{31}P-NMR (161.9 MHz, (D_6)acetone): −15.0 (*ddd*, ^1J(P,F) = 1004, ^3J(P,H_{eq}–C(5)) = 25.3, ^5J(P,H_{ax}–C(5)) ≈ 1). ^{19}F-NMR (376.5 MHz, (D_6)acetone): −86.4 (*d*, ^1J(F,P) = 1004). EI-MS: 285 (14, M^+), 194 (9, $[M - PhCH_2]^+$), 186 (14), 171 (19), 160 (23), 91 (100, $PhCH_2^+$), 77 (11, Ph^+).

*(−)-(1*S*,3*S*,6*R*)-7-Benzyl-3-fluoro-2,4-dioxa-7-aza-3-phosphadecalin 3-Oxide* (*=(−)-(2*S*,4a*R*,8a*S*)-2-Fluorohexahydro-5-(phenylmethyl)-4*H*-1,3,2-dioxaphosphorino[5,4-*b*]pyridine 2-Oxide*; (−)-**13a**): $[\alpha]_D^{25} = -72.8$ ($c = 0.29$, acetone). All other data: identical with those of (+)-**13a**.

*(+)-(1*R*,3*S*,6*S*)-7-Benzyl-3-fluoro-2,4-dioxa-7-aza-3-phosphadecalin 3-Oxide* (*=(+)-(2*S*,4a*S*,8a*R*)-2-Fluorohexahydro-5-(phenylmethyl)-4*H*-1,3,2-dioxaphosphorino[5,4-*b*]pyridine 2-Oxide*; (+)-**13b**): Colorless plates. M.p. 68.5–71° ((±)-**13b**: m.p. 86.0–90.5° [9]). R_f (hexane/Et_2O 1 : 2) 0.19. $[\alpha]_D^{25} = +91.9$ ($c = 0.27$, acetone). IR (KBr): identical with that of (±)-**13b** [9]. ^{1}H-NMR (400 MHz, (D_6)acetone): 7.36–7.22 (*m*, *Ph*CH_2); 4.97 (*A* of *ABX-P*, $^2J = 10.2$, ^3J(5eq,P) = 8.5, ^3J(5eq,6) = 5.5, H_{eq}–C(5))[23]; 4.55 (*sept.*-like, ^3J(1,10ax) ≈ ^3J(1,6) ≈ 10, ^3J(1,10eq) = 4.5, ^4J(1,F) = 3.5, ^3J(1,P) ≈ 1, H–C(1)); 4.49 (*B* of *ABX-P*, ^3J(5ax,P) = 14.5, $^2J = {}^3J$(5ax,6) = 10.3, ^4J(5ax,F) = 3.2, H_{ax}–C(5))[23]); 3.86, 3.28 (*AB*, $^2J = 13.6$, PhCH_2); 2.85 (*X* of *ABX*, ^3J(6,1) ≈ 10, ^3J(6,5ax) = 10.3, ^3J(6,5eq) = 5.5, ^5J(6,F) = 3.8, H–C(6)); 2.78 (*m*, *d*-like, $^2J \approx 12$, H_{eq}–C(8)); 2.21 (*m*, $w_{1/2} \approx 20$, H_{eq}–C(10)); 2.08 (*td*, $^2J = {}^3J$(8ax,9ax) = 11.9, ^3J(8ax,9eq) = 2.8, H_{ax}–C(8)); 1.72 (*m*, *d*-like, $w_{1/2} \approx 18$, $^2J \approx 11$, ^5J(9eq,P) ≈ 2, H_{eq}–C(9)); 1.63–1.50 (*m*, H_{ax}–C(9), H_{ax}–C(10)). ^{13}C-NMR (100.6 MHz, (D_6)acetone): 139.4 (C(1′)); 129.6 (C(3′), C(5′)); 129.3 (C(2′), C(6′)); 128.1 (C(4′)); 82.1 (*dd*, ^2J(1,P) = 6.3, ^3J(1,F) = 1.5, C(1)); 74.1 (*d*, ^2J(5,P) = 78.4, C(5)); 61.2 (*d*, ^3J(6,P) = 10.6, C(6)); 58.4 (Ph*C*H_2); 52.8 (C(8)); 32.0 (*d*, ^3J(10,P) = 7.6, C(10)); 23.5 (*d*, ^4J(9,P) = 2.3, C(9)). ^{31}P-NMR (161.9 MHz, (D_6)acetone): −14.1 (*d*br.*ddd*, ^1J(P,F) = 988, ^3J(P,H_{ax}–C(5)) = 14.5, ^3J(P,H_{eq}–C(5)) = 8.5, ^3J(P,1) ≈ 1, ^5J(P,9eq) ≈ 2)[23]). ^{19}F-NMR (376.5 MHz, (D_6)acetone): −71.2 (*dq*, ^1J(F,P) = 997, ^4J(F,H–C(1)) ≈ ^4J(F,H_{ax}–C(5)) ≈ ^5J(F,H–C(6)) ≈ 3). EI-MS: 285 (10, M^+), 194 (10, $[M - PhCH_2]^+$), 186 (12), 171 (16), 160 (22), 91 (100, $[PhCH_2]^+$), 77 (4) Ph^+).

---

[23]) The descriptors 'ax' and 'eq' for the H-atoms of CH_2(5) are based on their relative positions in the chair conformation of the 2,4-dioxa-3-phospha moiety. As discussed (*Scheme 5*), the conformation is rather a twist-boat (**TB-2**) than a chair in the *P(3)*-equatorially substituted compounds. For reasons of simplicity, the notation 'ax' and 'eq' is maintained. H_{ax}–C(5) is always *cis* to H–C(1) and H_{eq}–C(5) *trans* to H–C(1), see [18].

*(−)-(1*S*,3*R*,6*R*)-7-Benzyl-3-fluoro-2,4-dioxa-7-aza-3-phosphadecalin 3-Oxide* (*=(−)-(2*R*,4a*R*,8a*S*)-2-Fluorohexahydro-5-(phenylmethyl)-4*H*-1,3,2-dioxaphosphorino[5,4-*b*]pyridine 2-Oxide*; (−)-**13b**): $[\alpha]_D^{25} = -93.8$ ($c = 0.26$, acetone). All other data: identical with those of (+)-**13b**.

*(+)-(1*S*,3*S*,6*S*)-7-Benzyl-3-fluoro-2,4-dioxa-7-aza-3-phosphadecalin 3-Oxide* (*=(+)-(2*S*,4a*S*,8a*S*)-2-Fluorohexahydro-5-(phenylmethyl)-4*H*-1,3,2-dioxaphosphorino[5,4-*b*]pyridine 2-Oxide*; (+)-**14a**): Colorless prisms. M.p. 101.5–104° ((±)-**14a**: m.p. 107–110.5° [9]). R_f (hexane/AcOEt 1:1) 0.24. $[\alpha]_D^{25} = +58.5$ ($c = 0.38$, acetone). IR (KBr): identical with that of (±)-**14a** [9]. ^{1}H-NMR (400 MHz, (D_6)acetone): 7.43–7.22 (*m*, *Ph*CH_2); 5.05 (*A* of *ABX-P*, $^2J = 13.0$, ^3J(5eq,P) = 25.7, ^3J(5eq,6) = 1.6, H_{eq}–C(5)); 5.00 (*m*, $w_{1/2} \approx 8$, H–C(1)); 4.54 (*B* of *ABX-P*, $^2J = 13.0$, ^3J(5ax,6) = ^3J(5ax,P) = 1.5, H_{ax}–C(5)); 4.25, 3.27 (*AB*, $^2J = 13.8$, PhCH_2); 2.87 (*m*, *quint.*-like, $w_{1/2} \approx 15$, $^2J = 11.6$, H_{eq}–C(8)); 2.67 (*X* of *ABX-P*, ^3J(6,1) = ^3J(6,5ax) = ^3J(6,5eq) = ^4J(6,P) = 1.5, H–C(6)); 2.15 (*td*, $^2J = {}^3J$(8ax,9ax) = 12.2, ^3J(8ax,9eq) = 2.7, H_{ax}–C(8)); 2.02 (*m*, br. *d*-like, $w_{1/2} \approx 18$, H_{eq}–C(10)); 1.84 (*qt*, $^2J = {}^3J$(9ax,8ax) = ^3J(9ax,10ax) = 12.2, ^3J(9ax,8eq) = ^3J(9ax,10eq) = 3.8, H_{ax}–C(9)); 1.74 (*m*, $w_{1/2} \approx 30$, ^4J(10ax,P) = 7.1, H_{ax}–C(10)); 1.47 (*m*, *dq*-like, $w_{1/2} \approx 18$, $^2J = 12.2$, H_{eq}–C(9)). ^{13}C-NMR (100.6 MHz, (D_6)acetone): 139.8 (C(1′)); 129.7 (C(3′), C(5′)); 129.2 (C(2′), C(6′)); 127.9 (C(4′)); 81.5 (*d*, ^2J(1,P) = 7.7, C(1)); 70.4 (*dd*, ^2J(5,P) = 7.3, ^3J(5,F) < 1, C(5)); 58.9 (*d*, ^3J(6,P) = 5.3, C(6)); 57.5 (PhCH_2); 52.5 (C(8)); 30.7 (*d*, ^3J(10,P) = 8.8, C(10)); 20.5 (C(9)). ^{31}P-NMR (161.9 MHz, (D_6)acetone): −15.3 (*dddt*, ^1J(P,F) = 987, ^3J(P,H_{eq}–C(5)) = 25.7, ^4J(P,H_{ax}–C(10)) = 7.1, ^4J(P,H_{ax}–C(5)) = ^4J(P,6) = 1.5). ^{19}F-NMR (376.5 MHz, (D_6)acetone): −83.6 (*d*, ^1J(F,P) = 987). EI-MS: 285 (20, M^+), 194 (15, $[M - PhCH_2]^+$), 186 (15), 172 (21), 160 (34), 147 (22), 91 (100, $PhCH_2^+$), 65 (11).

*(−)-(1*R*,3*R*,6*R*)-7-Benzyl-3-fluoro-2,4-dioxa-7-aza-3-phosphadecalin 3-Oxide* (*=(+)-(2*R*,4a*R*,8a*R*)-2-Fluorohexahydro-5-(phenylmethyl)-4*H*-1,3,2-dioxaphosphorino[5,4-*b*]pyridine 2-Oxide*; (−)-**14a**): $[\alpha]_D^{25} = +59.8$ ($c = 0.36$, acetone). All other data identical with those of (+)-**14a**.

*(+)-(1*S*,3*R*,6*S*)-7-Benzyl-3-fluoro-2,4-dioxa-7-aza-3-phosphadecalin 3-Oxide* (*=(+)-(2*R*,4a*S*,8a*S*)-2-Fluorohexahydro-5-(phenylmethyl)-4*H*-1,3,2-dioxaphosphorino[5,4-*b*]pyridine 2-Oxide*; (+)-**14b**): Colorless oil ((±)-**14b**: colorless plates, m.p. 93–94.5° [9]). R_f (hexane/Et_2O 1:2) 0.26. $[\alpha]_D^{25} = +23.3$ ($c = 0.28$ acetone). IR (KBr): identical with that of (±)-**14b** [9]. ^{1}H-NMR (400 MHz, (D_6)acetone): 7.39–7.23 (*m*, *Ph*CH_2); 5.00 (*A* of *ABX-P*, $^2J = 11.8$, ^3J(5eq,P) = 10.9, ^3J(5eq,6) = 7.0, H_{eq}–C(5)); 4.95 (*ddd*, ^3J(1,P) = 12.8, ^3J(1,6) = 3.4, ^4J(1,F) = 2.7, H–C(1)); 4.62 (*B* of *ABX-P*, $^2J = 11.8$, ^3J(5ax,P) = 14.0, ^3J(5ax,6) = 3.4, ^4J(5ax,F) = 2.3, H_{ax}–C(5)); 4.04, 3.59 (*AB*, $^2J = 13.7$, PhCH_2); 3.21 (*X* of *ABX-P*, ^3J(6,5eq) = 6.8, ^3J(6,5ax) = ^3J(6,1) = 3.5, ^4J(6,P) = 1.8, H–C(6)); 2.72 (*ddd*, $^2J = 12.0$, ^3J(8eq,9ax) = 7.4, ^3J(8ax,9eq) = 3.6, H_{ax}–C(8)); 2.31 (*ddd*-like, $^2J = 12.0$, ^3J(8ax,9eq) = 7.7, ^3J(8eq,9ax) = 3.3, H_{ax}–C(8)); 2.06 (*m*, $w_{1/2} \approx 20$, H_{eq}–C(10)); 1.99–1.90 (*m*, H_{ax}–C(10)); 1.62–1.52 (*m*, CH_2(9)). ^{13}C-NMR (100.6 MHz, (D_6)acetone): 139.8 (C(1′)); 129.4 (C(3′), C(5′)); 129.3 (C(2′), C(6′)); 128.0 (C(4′)); 81.7 (*dd*, ^2J(1,P) = 8.8, ^3J(1,F) = 1.2, C(1)); 67.7 (*d*, ^2J(5,P) = 6.8, C(5)); 58.5 (PhCH_2); 57.0 (*d*, ^3J(6,P) = 9.0, C(6)); 49.0 (C(8)); 28.8 (*d*, ^3J(10,P) = 2.7, C(10)); 22.3 (C(9)). ^{31}P-NMR (161.9 MHz, (D_6)acetone): −15.6 (*dddddd*, ^1J(P,F) = 990, ^3J(P,H_{ax}–C(5)) = 14.0, ^3J(P,H–C(1)) = 12.8, ^3J(P,H_{eq}–C(5)) = 10.9, ^4J(P,H_{ax}–C(10)) = 3.4, ^4J(P,6) = 1.8)[23]. ^{19}F-NMR (376.5 MHz, (D_6)acetone): −74.5 (*m*, *dq*-like, ^1J(F,P) = 990, ^4J(F,H–C(1)) ≈ ^4J(F,H_{ax}–C(5)) ≈ ^4J(F,H_{eq}–C(5)) ≈ ^5J(F,H_{eq}–C(10)) ≈ 2). EI-MS: 285 (25, M^+), 194 (13, $[M - PhCH_2]^+$), 186 (15), 172 (22), 160 (41), 91 (100, $PhCH_2^+$), 65 (11).

*(−)-(1*R*,3*S*,6*R*)-7-Benzyl-3-fluoro-2,4-dioxa-7-aza-3-phosphadecalin 3-Oxide* (*=(−)-(2*S*,4a*R*,8a*R*)-2-Fluorohexahydro-5-(phenylmethyl)-4*H*-1,3,2-dioxaphosphorino[5,4-*b*]pyridine 2-Oxide*; (−)-**14b**): $[\alpha]_D^{25} = -22.4$ ($c = 0.27$, acetone). All other data: identical with those of (+)-**14b**.

5. *X-Ray Crystal-Structure Determinations of (−)-***13a** *and (+)-***14a**[16]). 5.1. *General.* All measurements were made with a *Nonius-KappaCCD* area-detector diffractometer [25], graphite-monochromated MoK_α radiation (λ 0.71073 Å), and an *Oxford-Cryosystems-Cryostream-700* cooler. Data reduction was performed with HKL DENZO and SCALEPACK [26]. The intensities were corrected for *Lorentz* and polarization effects, and an absorption correction based on the multi-scan method [27] was applied. The space groups were uniquely determined by the systematic absences. Equivalent reflections, other than *Friedel* pairs, were merged. Neutral-atom scattering factors for non-H-atoms were taken from [28] and the scattering factors for H-atoms were taken from [29]. Anomalous dispersion effects were included in F_c [30]; the values for f' and f'' were those of [31]. The values of the mass

attenuation coefficients were those of [32]. All calculations were performed with the SHELXL97 program [33], and the crystallographic diagrams were drawn with ORTEPII [34].

5.2. *Determination of (−)*-**13a** *and (+)*-**14a**. The unit-cell constants and an orientation matrix for data collection were obtained from a least-squares refinement of the setting angles of 66907 ((−)-**13a**) and 14905 ((+)-**14a**) reflections in the range $4° < 2\theta < 56°$ and $4° < 2\theta < 60°$, resp. The mosaicity was 0.602(1)° ((−)-**13a**) and 0.432(1)° ((+)-**14a**). A total of 295 ((−)-**13a**) and 240 ((+)-**14a**) frames were collected by using ω scans with κ offsets, 22 and 38 s exposure time and a rotation angle of 1.5° and 2.0° per frame, and a crystal-detector distance of 32.0 and 30.0 mm, resp. The data collection and refinement parameters are given in *Table 2*. A view of the molecules is shown in *Fig. 2* ((−)-**13a**) and *3* ((+)-**14a**). The structure were solved by direct methods with SIR92 [35], which revealed the positions of all non-H-atoms. There were three symmetry-independent molecules of the same enantiomer in the asymmetric unit of (−)-**13a**; the atomic coordinates of the two molecules were tested carefully for a relationship from a higher symmetry space group with the program PLATON [36], but none could be found; the molecules had very similar conformations with only small differences in the orientation of the phenyl ring. The non-H-atoms were refined anisotropically. All of the H-atoms were placed in geometrically calculated positions and refined by using a riding model where each H-atom was assigned a fixed isotropic displacement parameter with a value equal to 1.2 U_{eq} of its parent atom. The refinement of the structures was carried out on F^2 by using full-matrix least-squares procedures, which minimized the function $\Sigma w(F_o^2 - F_c^2)^2$. The weighting scheme was based on counting statistics and included a factor to downweight the intense reflections. Plots of $\Sigma w(F_o^2 - F_c^2)^2$ *vs.* $F_c/F_c(\max)$ and resolution showed no unusual trends. A correction for secondary extinction was applied. Refinement of the absolute structure parameter [37] yielded a value of −0.05(8) ((−)-**13a**) and 0.02(8) ((+)-**14a**), which confidently confirmed that the refined models corresponded with the true enantiomorphs.

6. *Enzyme Kinetics*. 6.1. *General*. For the detailed experimental procedure and the methods of data analysis, see the preceding reports [1][2]. The following parameters were as in [1]: Apparatus and general experimental conditions, phosphate buffer pH 7.00, AChE soln., ATC and DTNB solns., inhibitor solns., and the determination of K_m. P(O)F(O^iPr)$_2$ (diisopropyl phosphorofluoridate) was used as the standard reference.

6.2. Ellman-*Assay* [20]. In a polystyrene cell (4 ml, $d = 1$ cm), phosphate buffer pH 7.00 (2 ml), DTNB soln. (100 µl), and ATC soln. (20 µl) were mixed and thermostatted at 25° (*ca.* 5 min). Then, inhibitor soln. (x µl, known [***I***], $x \leq 25$ µl) and MeCN ($(25 - x)$ µl) were added. At $t = 0$, the AChE soln. (1 ml) was added and the mixture gently mixed for 10 s. After 20 s, the monitoring of the absorption at 412 ± 2 nm (liberated bis-anion of 5-mercapto-2-nitrobenzoic acid) automatically started, and 600 data points were collected for 10 min at various concentrations of the inhibitor. As in the K_m determinations, the total volume was 3.145 µl, the concentration of the substrate [***S***] = 502 µM. Per inhibitor, at least five measurements with different inhibitor concentrations were performed, the smallest one being *ca.* 1/5 – 1/10 of the largest one.

6.3. *Data Analysis* [21]. The integrated rate equation describing product generation (monitored by the absorbance A at 412 ± 2 nm) and the apparent rate constants (k_{obs}) is given by *Eqn. 1*. It was fitted ($R > 0.999$) to progress curves recorded at fixed [***S***] and variable [***I***] (primary plot, $A = f(t)$) to obtain a series of k_{obs} values and their standard errors (SE). The inhibition parameters were obtained from the secondary plots ($k_{obs} = f([\boldsymbol{I}])$) that resulted from weighted (SE^{-2}) linear or nonlinear regression according to *Eqns. 2* or *3*. The analysis of these plots enabled a differentiation between the inhibition mechanisms: k_{obs} depended linearly upon the inhibitor concentration for mechanism *a* and hyperbolically for mechanism *b* (see *Scheme 6*). For mechanism *a*, the k_a values were calculated according to *Eqn. 2*, its slope $k_{obs}/[\boldsymbol{I}]$ was obtained from the linear regression. The decisive plot for mechanism *b* was doubly reciprocal ($1/k_{obs} = f(1/[\boldsymbol{I}])$, *Eqn. 3*), and the K_D- and k_p-values were calculated by linear regression, the slope being $(K_D/k_p)(1 + [\boldsymbol{S}]/K_m)$ and the intercept $1/k_p$. The overall inhibitory potency (k_i) is expressed by k_p/K_D (see *Scheme 6*).

$$A = \frac{v_z}{k_{obs}}\left(1 - e^{-k_{obs} \cdot t}\right) \tag{1}$$

Table 2. *Crystallographic Data of (−)-***13a** *and (+)-***14a**

	(−)-**13a**	(+)-**14a**
Crystallized from	Et_2O	pentane/Et_2O
Empirical formula	$C_{13}H_{17}FNO_3P$	$C_{13}H_{17}FNO_3P$
M_r	285.25	285.25
Crystal color, habit	colorless, prism	colorless, prism
Crystal dimensions [mm]	$0.25 \times 0.35 \times 0.35$	$0.15 \times 0.22 \times 0.25$
Temperature [K]	160(1)	160(1)
Crystal system	orthorhombic	orthorhombic
Space group	$P2_12_12_1$ (#19)	$P2_12_12_1$ (#19)
Z	12	4
Reflections for cell determination	66907	14905
2θ range for cell determination [°]	4–56	4–60
Unit cell parameters: a [Å]	13.5669(2)	9.7745(2)
b [Å]	15.5403(2)	10.0774(2)
c [Å]	19.7914(3)	13.5432(2)
V [Å^3]	4172.7(1)	1334.03(4)
$F(000)$	1800	600
D_x [g cm^{-3}]	1.362	1.420
$\mu(\mathrm{Mo}K_\alpha)$ [mm^{-1}]	0.212	0.221
Scan type	ω	ϕ and ω
$2\theta_{(\max)}$ [°]	56	60
Transmission factors (min; max)	0.812; 0.951	0.854; 0.970
Total reflections measured	62660	24752
Symmetry independent reflections	9854	3878
R_{int}	0.082	0.063
Reflections with $I > 2\sigma(I)$	8055	3449
Reflections used in refinement	9854	3878
Parameters refined	515	173
Final $R(F)$ ($I > 2\sigma(I)$ reflections)	0.0541	0.0383
$wR(F^2)$ (all data)	0.1346	0.0958
Weights	$w = [\sigma^2(F_o^2) + (0.073P)^2 + 0.4328P]^{-1}$, where $P = (F_o^2 + 2F_c^2)/3$	$w = [\sigma^2(F_o^2) + (0.0543P)^2 + 0.1646P]^{-1}$, where $P = (F_o^2 + 2F_c^2)/3$
Goodness of fit	1.079	1.068
Secondary extinction coefficient	0.0107(9)	0.020(2)
Final Δ_{max}/σ	0.001	0.001
$\Delta\rho$ (max; min) [e Å^{-3}]	0.59; −0.56	0.34; −0.30
$\sigma(d_{(C-C)})$ [Å]	0.003–0.005	0.002–0.003

$$k_a = \left(\frac{k_{obs}}{[I]}\right)\left(1 + \frac{[S]}{K_m}\right) \tag{2}$$

$$\frac{1}{k_{obs}} = \left(\frac{K_D}{k_p}\right)\left(1 + \frac{[S]}{K_m}\right)\left(\frac{1}{[I]}\right) + \frac{1}{k_p} \tag{3}$$

6.4. *Results* (*Table 1*). The secondary plot ($k_{obs} = f([\boldsymbol{I}])$) exhibited a linear dependence for (±)-**13a**, (+)- and (−)-**13a**, (+)- and (−)-**14a**, and P(O)F(O^{i}Pr)$_2$. Hence, mechanism *a* was assigned. In the case of (+)- and (−)-**13b**, and (+)- and (−)-**14b**, the secondary plot depended hyperbolically upon [***I***], and mechanism *b* was assigned to these compounds.

REFERENCES

[1] P. Lorenzetto, M. Wächter, P. Rüedi, *Helv. Chim. Acta* **2011**, *94*, 746.
[2] C. Clerc, P. Rüedi, *Helv. Chim. Acta* **2012**, *95*, 17.
[3] M. Wächter, P. Rüedi, *Chem. Biodiversity* **2009**, *6*, 283.
[4] M. Wächter, 'Herstellung von optisch aktiven Organophosphaten mit *cis*- und *trans*-Decalingerüst zur Untersuchung der Inhibition von Acetylcholinesterase mittels Enzymkinetik und ^{31}P-NMR Spektroskopie', Ph.D. Thesis, University of Zurich, 2009.
[5] S. Furegati, F. Gorla, A. Linden, P. Rüedi, *Chem.-Biol. Interact.* **2005**, *157–158*, 415.
[6] W. Ganci, E. J. M. Meier, F. A. Merckling, G. Przibille, U. Ringeisen, P. Rüedi, *Helv. Chim. Acta* **1997**, *80*, 421; S. Furegati, W. Ganci, G. Przibille, P. Rüedi, *Helv. Chim. Acta* **1998**, *81*, 1127.
[7] M. J. Stöckli, P. Rüedi, *Helv. Chim. Acta* **2001**, *84*, 106; M. J. Stöckli, P. Rüedi, *Helv. Chim. Acta* **2007**, *90*, 2058.
[8] S. Furegati, O. Zerbe, P. Rüedi, *Chem.-Biol. Interact.* **2005**, *157–158*, 418.
[9] S. Furegati, W. Ganci, F. Gorla, U. Ringeisen, P. Rüedi, *Helv. Chim. Acta* **2004**, *87*, 2629.
[10] J. A. Dale, D. L. Dull, H. S. Mosher, *J. Org. Chem.* **1969**, *34*, 2543; G. R. Sullivan, J. A. Dale, H. S. Mosher, *J. Org. Chem.* **1973**, *38*, 2143; J. A. Dale, H. S. Mosher, *J. Am. Chem. Soc.* **1973**, *95*, 512; I. Ohtani, T. Kusumi, Y. Kahman, H. Kakisawa, *J. Am. Chem. Soc.* **1991**, *113*, 4092.
[11] C. Clerc, I. Matarazzo, P. Rüedi, *Helv. Chim. Acta* **2009**, *92*, 14.
[12] S. Hashimoto, H. Setoi, S. Takeno, H. Kayakiriv, A. A. Richiyaado, to *Fujisawa Pharmaceutical Company, Ltd.*, Jpn. Kokai Tokkyo Koho, JP 61122269, A 1985000255725, 10.06.1986.
[13] M. Mocerino, R. V. Stick, *Austr. J. Chem.* **1990**, *43*, 1183; D. Enders, U. Jegelka, *Synlett* **1992**, 999; M. H. Haukaas, G. A. O'Doherty, *Org. Lett.* **2001**, *3*, 401; Y. Banba, C. Abe, H. Nemoto, A. Kato, I. Adachi, H. Takahata, *Tetrahedron: Asymmetry* **2001**, *12*, 817; H. Takahata, Y. Banba, H. Ouchi, H. Nemoto, A. Kato, I. Adachi, *J. Org. Chem.* **2003**, *68*, 3603; H. Takahata, Y. Banba, H. Ouchi, H. Nemoto, *Org. Lett.* **2003**, *5*, 2527; H. Takahata, Y. Banba, M. Sasatani, H. Nemoto, A. Kato, I. Adachi, *Tetrahedron* **2004**, *60*, 8199; I. S. Kim, J. S. Oh, O. P. Zee, Y. H. Jung, *Tetrahedron* **2007**, *63*, 2622; J. M. Andrés, R. Pedrosa, A. Pérez-Encabo, *Eur. J. Org. Chem.* **2007**, 1803; N. B. Kalamkar, V. M. Kasture, D. D. Dhavale, *J. Org. Chem.* **2008**, *73*, 3619; B. Wang, R.-H. Liu, *Eur. J. Org. Chem.* **2009**, 2845; R. Rengasamy, M. J. Curtis-Long, H.-W. Ryu, K.-Y. Oh, K.-H. Park, *Bull. Korean Chem. Soc.* **2009**, *30*, 1531.
[14] R. J. B. H. N. van den Berg, T. Wennekes, A. Ghisaidoobe, W. E. Donker-Koopman, A. Strijland, R. G. Boot, G. A. van der Marel, J. M. F. G. Aerts, H. S. Overkleeft, *ACS Med. Chem. Lett.* **2011**, *2*, 519.
[15] D. W. Knight, N. Lewis, A. C. Share, D. Haigh, *J. Org. Chem., Perkin Trans. 1* **1998**, 3673; P. Kumar, M. S. Bodas, *J. Org. Chem.* **2005**, *70*, 360; P. S. Kumar, G. D. K. Kumar, S. Baskaran, *Eur. J. Org. Chem.* **2008**, 6063; W.-H. Chiou, G.-H. Lin, C.-W. Liang, *J. Org. Chem.* **2010**, *75*, 1748; H. P. Kokatla, R. Lahiri, P. K. Kancharla, V. R. Doddi, I. D. Vankar, *J. Org. Chem.* **2010**, *75*, 4608; S. P. Chavan, K. R. Harale, N. B. Dumare, U. R. Kalkote, *Tetrahedron: Asymmetry* **2011**, *22*, 587.
[16] A. Jourdant, J. Zhu, *Tetrahedron Lett.* **2000**, *41*, 7033.
[17] P. A. Lorenzetto, A. Strehler, P. Rüedi, *Helv. Chim. Acta* **2006**, *89*, 3023.
[18] S. Furegati, M. Binder, A. Linden, P. Rüedi, *Helv. Chim. Acta* **2006**, *89*, 1351.
[19] M. Wächter, S. Jurt, A. Linden, P. Rüedi, in preparation.
[20] G. L. Ellman, K .D. Courtney, V. Andres Jr., R. M. Featherstone, *Biochem. Pharmacol.* **1961**, *7*, 88.
[21] A. Baici, *Biol. Chem.* **1998**, *379*, 1007.
[22] A. Baici, P. Schenker, M. Wächter, P. Rüedi, *Chem. Biodiversity* **2009**, *6*, 261.
[23] M. Wächter, P. Rüedi, in preparation.
[24] C. J. Wilkins, *J. Chem. Soc.* **1951**, 2726.
[25] R. Hooft, KappaCCD Collect Software, Nonius BV, Delft, The Netherlands, 1999.
[26] Z. Otwinowski, W. Minor, 'Macromolecular Crystallography, Part A', in 'Methods in Enzymology', Vol. 276, Eds. C. W. Carter Jr., R. M. Sweet, Academic Press, New York, 1997, p. 307.
[27] R. H. Blessing, *Acta Crystallogr., Sect. A* **1995**, *51*, 33.

[28] E. N. Maslen, A. G. Fox, M. A. O'Keefe, in 'International Tables for Crystallography', Ed. A. J. C. Wilson, Kluwer Academic Publishers, Dordrecht, 1992, Vol. C, Table 6.1.1.1, p. 477.
[29] R. F. Stewart, E. R. Davidson, W. T. Simpson, *J. Chem. Phys.* **1965**, *42*, 3175.
[30] J. A. Ibers, W. C. Hamilton, *Acta Crystallogr.* **1964**, *17*, 781.
[31] D. C. Creagh, W. J. McAuley, in 'International Tables for Crystallography', Ed. A. J. C. Wilson, Kluwer Academic Publishers, Dordrecht, 1992, Vol. C, Table 4.2.6.8, p. 219.
[32] D. C. Creagh, J. H. Hubbell, in 'International Tables for Crystallography', Ed. A. J. C. Wilson, Kluwer Academic Publishers, Dordrecht, 1992, Vol. C, Table 4.2.4.3, p. 200.
[33] G. M. Sheldrick, 'SHELXL97, Program for the Refinement of Crystal Structures', University of Göttingen, Germany, 1997.
[34] C. K. Johnson, 'ORTEPII', Report ORNL-5138, Oak Ridge National Laboratory, Oak Ridge, Tennessee, 1976.
[35] A. Altomare, G. Cascarano, C. Giacovazzo, A. Guagliardi, M. C. Burla, G. Polidori, M. Camalli, 'SIR92', *J. Appl. Crystallogr.* **1994**, *27*, 435.
[36] A. L. Spek, 'PLATON, Program for the Analysis of Molecular Geometry', University of Utrecht, The Netherlands, 2006.
[37] H. D. Flack, G. Bernardinelli, *Acta Crystallogr., Sect. A* **1999**, *55*, 908; H. D. Flack, G. Bernardinelli, *J. Appl. Crystallogr.* **2000**, *33*, 1143.

Received December 15, 2011